Environmental Modelling and Software 181 (2024) 106187

Contents lists available at ScienceDirect

Environmental Modelling and Software

journal homepage: www.elsevier.com/locate/envsoft

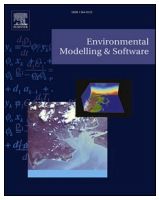

PyCHAMP: A crop-hydrological-agent modeling platform for groundwater management

Chung-Yi Lin [a], Maria Elena Orduna Alegria [b], Sameer Dhakal [a], Sam Zipper [b,c], Landon Marston [a,*]

[a] The Charles Edward Via, Jr. Department of Civil and Environmental Engineering, Virginia Tech, Blacksburg, VA, 24061, USA
[b] Kansas Geological Survey, University of Kansas, Lawrence, KS, 66047, USA
[c] Department of Geology, University of Kansas, Lawrence, KS, 66047, USA

ARTICLE INFO

Keywords:
Agent-based modeling
Water conservation
Coupled human and natural systems
Socio-hydrology
Social-ecological systems
Agriculture

ABSTRACT

The Crop-Hydrological-Agent Modeling Platform (PyCHAMP) is a Python-based open-source package designed for modeling agro-hydrological systems. The modular design, incorporating aquifer, crop field, groundwater well, finance, and behavior components, enables users to simulate and analyze the interactions between human and natural systems, considering both environmental and socio-economic factors. This study demonstrates PyCHAMP's capabilities by simulating the dynamics in the Sheridan 6 Local Enhanced Management Area, a groundwater conservation program in the High Plains Aquifer in Kansas. We highlight how a model, empowered by PyCHAMP, accurately captures human-water dynamics, including groundwater level, water withdrawal, and the fraction of cropland dedicated to each crop. We also show how farmer behavior, and its representation, drives system outcomes more strongly than environmental conditions. The results indicate PyCHAMP's potential as a useful tool for human-water research and sustainable groundwater management, offering prospects for future integration with detailed sub-models and systematic evaluation of model structural uncertainty.

1. Introduction

The investigation of the interconnection between human actions and the natural world is crucial for addressing complex management challenges. The study of this interconnection is known by many names in literature, including coupled human and natural systems (CHANS; Liu et al., 2007), socio-hydrology (Sivapalan et al., 2012), social-ecological systems (SES; Ostrom, 2009), hydro-economic modeling (Harou et al., 2009), and multi-sector dynamics (Reed et al., 2022). These research communities focus on the multifaceted drivers and feedback mechanisms that define interactions between humans and nature with the goal of improving sustainable environmental management. Understanding the interconnection of human-natural systems has been instrumental in refining policy evaluation related to incentives (Lin et al., 2023), advancing integrated resource management strategies (Berglund, 2015; Schrieks et al., 2021), enhancing disaster risk reduction plans (Han et al., 2022), and fostering sustainable development (Castro et al., 2020; Savin et al., 2023; Zhang et al., 2024).

In the context of sustainable groundwater management, a major part of the world's food production depends on irrigation from groundwater (Mukherjee et al., 2021). Increasing population (Lall et al., 2020), expansion of irrigated cropland (Bhattarai et al., 2021), and changing climate (Taylor et al., 2013) all combine to intensify groundwater depletion (Jasechko et al., 2024), leading to calls for greater water conservation (Aeschbach-Hertig and Gleeson, 2012). However, increased groundwater demand often leads to the tragedy of the commons (Ostrom, 1990), where individual users, acting independently according to their self-interest, overuse and deplete a shared resource like groundwater, ultimately harming the resource's long-term sustainability. These complex human-nature interactions leading to aquifer depletion highlight the need to incorporate the dynamics of human-natural systems into sustainable groundwater management, where farmers sharing a common aquifer respond to each other's water use. Factors such as crop choice, irrigation methods, climate conditions, and water rights influence these behaviors, reflecting the complexities of broader human-natural systems.

* Corresponding author.
E-mail addresses: chungyi@vt.edu (C.-Y. Lin), malena.orduna@ku.edu (M.E. Orduna Alegria), sameerdhakal@vt.edu (S. Dhakal), samzipper@ku.edu (S. Zipper), lmarston@vt.edu (L. Marston).

https://doi.org/10.1016/j.envsoft.2024.106187
Received 16 April 2024; Received in revised form 2 July 2024; Accepted 12 August 2024
Available online 13 August 2024

However, most groundwater sustainability modeling efforts treat human decisions as fixed boundary conditions. Rather than simulating them endogenously, these models do not account for dynamic feedback between human and natural systems. For example, Malekinezhad and Banadkooki (2017) studied the impact of climate change and human pressures on an aquifer using MODFLOW (Harbaugh, 2005), where the water requirements of cultivated areas are a time series input to MODFLOW. The global hydrological model PCR-GLOBWB (Sutanudjaja et al., 2018) has an irrigation and water use module to simulate human activity, but the water demands are also derived from input data, such as climate and population. Studies that adopted PCR-GLOBWB cannot endogenously simulate the active human decisions and their interactions with the natural environment (Wada et al., 2016; Wu et al., 2024). The diverse and complex nature of individual farming decisions, influenced by environmental and socio-economic factors, highlights the variability and complexity inherent in human-natural systems. This suggests a need for more versatile modeling approaches to better accommodate the nuanced and varied aspects of these systems (Gorelick and Zheng, 2015; Hrozencik et al., 2017).

Agent-based modeling (ABM), a bottom-up modeling approach, shows great promise in capturing the interactions among heterogeneous natural and human agents (Kaiser et al., 2020; Zellner, 2008). Here, we define agents to be entities with unique attributes and behavioral rules like farmers, aquifers, well infrastructures, crop fields, and economic markets. Agent-based modeling has informed groundwater management on scales and dimensions not feasible with traditional fieldwork, including the assessment of social tipping points in global groundwater management (Castilla-Rho et al., 2017), analysis of groundwater markets (Aghaie et al., 2020b; Zolfagharipoor and Ahmadi, 2021), investigation of land-use changes based on farmers' characteristics (Holtz and Pahl-Wostl, 2012), and the exploration of groundwater management strategies under climate change scenarios (Al-Amin et al., 2015).

However, developing a complex model endogenously considering human and natural dimensions is a challenging task (An et al., 2021) that demands considerable effort to conceptually and technically establish information flow among agents and various sub-models. For instance, Castilla-Rho et al. (2015) integrated groundwater flow equations into NetLogo (Wilensky, 1999) with their FlowLogo model, while Jaxa-Rozen et al. (2019) linked NetLogo with MODFLOW/SEAWAT models for more accurate geohydrological representations, including contaminant transport in aquifers. More recently, Nozari et al. (2023) integrated DSSAT, MODFLOW, and ABM to form an agent-based hydro-economic model targeting a region overlying the northwest High Plains Aquifer. Additionally, a recent review by Canales et al. (2024) provides a summary of efforts to couple groundwater models with human models framed as ABM.

Although the modeling frameworks discussed in the literature are generally user-friendly, allowing users to create simulation models with corresponding input files, the selected sub-models and information flows (coupling structures) are typically not designed to be substituted or altered, which could potentially limit their application or further extension. Pynsim, a Python package developed by Knox et al. (2018), addresses this gap. Demonstrated in Jordan case studies (Avisse et al., 2020; Klassert et al., 2023), Pynsim enables users to create a node-link network topology for customizing information flows among nodes. However, it heavily relies on users' technical experience to populate each node with customized scripts or sub-models.

Our study aims to develop the Crop-Hydrological-Agent Modeling Platform (PyCHAMP), a Python-based platform built on the MESA agent-based modeling framework (Masad and Kazil, 2015). Designed to enhance agricultural groundwater management modeling, PyCHAMP features predefined components that reduce the technical skill requirements while retaining flexibility for users to customize Python scripts and sub-models (e.g., agent types). These components include aquifers, crop fields, groundwater wells, finance, and behavioral actors (i.e., farmers), as detailed in Section 2.1. The primary contribution of PyCHAMP is its ability to serve as a container for both default and customized 1) agent types that can vary in complexity and simulation timestep and 2) models different in simulation procedures or coupling structures. This versatility of PyCHAMP improves the code's reusability and expandability – a major challenge in agent-based modeling (Daly et al., 2022) - by minimizing technical skill requirements needed to use the platform. PyCHAMP does this by using built-in models while allowing experienced users to populate PyCHAMP by developing new agent types and models.

Within PyCHAMP, users have two main options: 1) select a model and substitute different agent types registered in PyCHAMP or compare different network topologies by modifying input files without additional technical programming, or 2) develop a new model with a customized simulation procedure using PyCHAMP, following the Mesa protocol. These features facilitate the comparison of model structures, including complexity, network topology, and social-behavioral theories. They also enhance control over computational costs and model output uncertainty, addressing key aspects highlighted in recent research (Lin and Yang, 2022; Srikrishnan and Keller, 2021; Sun et al., 2016).

The Sheridan 6 Local Enhanced Management Area (SD-6 LEMA) in western Kansas is used as our case study. Two key objectives of the case study are 1) demonstrating how to apply PyCHAMP, including parameterization, components connectivity, and result analysis and interpretation and 2) illustrating the impact of network topology changes through adjustments in input files. In the SD-6 LEMA example, the CONSUMAT behavioral framework (Jager et al., 1999) is assumed to depict farmers' behaviors, though other behavioral frameworks could be adopted by users of PyCHAMP. We will discuss other features of PyCHAMP and its future directions in Section 5. Overall, PyCHAMP represents a significant advancement in environmental management and modeling, linking individual decision-making to broader environmental outcomes through a platform derived from Mesa.

2. Methods

2.1. PyCHAMP

The Crop-Hydrological-Agent Modeling Platform (PyCHAMP) is an open-source Python package designed to analyze policies and assess decision-making processes in agro-hydrological systems with complex human-natural interplay. PyCHAMP is organized into five core components: aquifer, field, well, finance, and behavior. Each component serves as a container to accommodate corresponding agent types. A component in PyCHAMP is called a module, which refers to a file containing Python statements and definitions, such as those for classes and functions. An agent type is programed as a class, which serves as a template for creating objects (i.e., agents), encapsulating both attributes (data) and methods (functions) for the objects. PyCHAMP includes five default agent types (classes) for each corresponding component (module): Aquifer, Field, Well, Finance, and Behavior, as illustrated in Fig. 1. An additional Optimization class is provided to enhance flexibility in programming agent types. PyCHAMP also comes with a model module to store developed models. Currently, a SD-6 model that we built for the SD-6 LEMA case study (Section 3) is available.

The development of PyCHAMP is based on the Mesa ABM framework (Masad and Kazil, 2015), a comprehensive and well-supported Python 3-based framework that enables the rapid development of agent-based models. The primary requirement for customizing agent types and models within PyCHAMP is that they must inherit the basic agent (i.e., *Mesa.Agent*) and model (i.e., *Mesa.Model*) classes from Mesa, as detailed in our online manual. The outputs of each agent type are fully user-defined and often linked to a specific model design. Adopting Mesa offers several advantages: i) it provides modularized features such as *schedulers* and a browser-based interface for visualizations and ii) integrates seamlessly with Python's robust data analysis capabilities (e.g., *datacollector*). The use of Mesa not only highlights PyCHAMP's

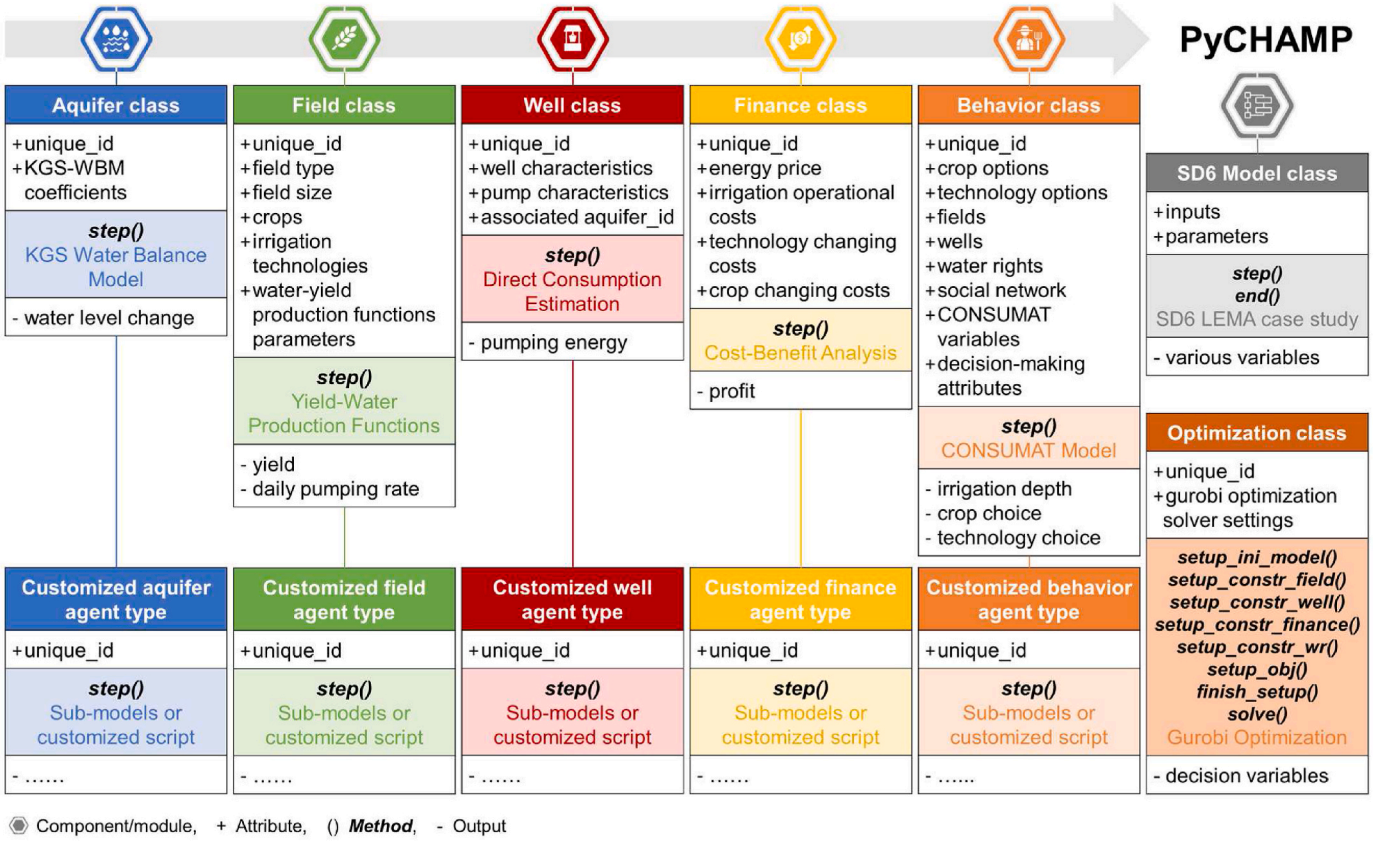

Fig. 1. Class diagram for PyCHAMP. The symbols +, (), and - represent a class's attributes, methods, and core outputs, respectively. Customized agent types can be added into corresponding PyCHAMP components (modules). The PyCHAMP online manual (http://dises-pychamp.readthedocs.io/) provides further documentation detailing the different components/modules.

compatibility with the expanding Python scientific ecosystem but also establishes PyCHAMP as a versatile platform ready for future development extensions and integrations with other Python scripts and sub-models.

Each default class (i.e., agent type) within PyCHAMP is crafted to perform specific functions, outputting variables to fit the designed information flow of the SD-6 Model (Section 3.2): Aquifer, Field, and Well classes employ distinct statistical relationships to evaluate changes in groundwater levels, crop yields, and the energy demands of groundwater pumping, respectively. The Finance class is designed with attributes related to pricing and costs, facilitating the computation of profits based on various farming practices and the resultant crop yields. The Behavior class focuses on modeling farmers' decision-making. Decision-making within PyCHAMP is governed by a rule-based behavioral framework, CONSUMAT (Jager et al., 1999), as it integrates multiple commonly used psychological and economic theories (e.g., Theory of Planned Behavior; Ajzen, 1991) into a single framework and has been successfully used in the literature to describe farmers' behaviors (Acosta-Michlik and Espaldon, 2008; Mialhe et al., 2012; Vinh et al., 2005). The decisions made under each associated CONSUMAT state are framed as an optimization problem with different inputs, addressed through the Optimization class (detailed in Section 2.1.5), where the Gurobi optimization solver is employed. The functionalities and applications of each module and class are explained in the following sections, with Section 2.2 focusing on employing PyCHAMP to simulate complex interactions within human-natural systems.

Below, we first describe the general structure of PyCHAMP and the types of data used to parameterize agent types for the corresponding components. We then demonstrate the use of PyCHAMP through a specific case study, where we detail the data and parameters specific to that case.

2.1.1. Aquifer component

The aquifer component (module) is designed to simulate the change in groundwater levels at each timestep. Currently, the supported agent type in the aquifer component is called Aquifer class. The Aquifer class simulates the annual groundwater level change using the Kansas Geological Survey–Water Balance Method (Butler et al., 2018):

$$\Delta WL = \frac{I}{Area \times S_y} - \frac{Q}{Area \times S_y} \approx b_{aq} - a_{aq} Q \tag{1}$$

where ΔWL is the annual groundwater level change [m], I is net inflow [m^3], and Q is the annual pumping amount [m^3]. The term S_y is the specific yield [-] and $Area$ represents the area of the aquifer [m^2]. For the groundwater-dependent regions where S_y and I have negligible change over time, like our SD-6 LEMA study area, we can represent $\frac{I}{Area \times S_y}$ and $\frac{1}{Area \times S_y}$ with a_{aq} and b_{aq}, respectively. The coefficients, a_{aq} and b_{aq}, can be estimated by linear regression on the annual groundwater level change and water pumping data (Butler et al., 2018). The saturated thickness ST [m]) of an aquifer can then be updated by:

$$ST_t = ST_{t-1} + \Delta WL_{t-1} \tag{2}$$

where t represents a timestep of one year. The initial saturated thickness (ST_0 [m]) is given as an input. The Kansas Geological Survey-Water Balance Method is a parsimonious approach for simulating the aquifer response to pumping which is appropriate for our study region due to the deep-water tables, relatively constant net inflows through time, and relatively homogeneous aquifer conditions (Butler et al., 2020, 2023).

2.1.2. Field component

The field component (module) is structured to simulate crop yields and daily pumping rates at each annual time step. The agent type currently available inside the field component is called Field class. The Field class simulates the crop growth through empirical water-yield production functions, a concept shown in (English et al., 2002), and estimates the daily pumping rate from the annual withdrawal by a linear relationship (McCarthy et al., 2020). Water-yield production functions assume that the yield will increase with the amount of the applied water; however, the yield will gradually decrease after reaching the optimal amount of applied water (Fig. 2). The function can be estimated by fitting the water-yield parabola to the observed crop yield and the applied water data. The applied water (AW_c [cm]) is the total irrigation amount plus precipitation during the growing season. When applying the water-yield production functions in a simulation, the irrigation amount is determined through farmers' decisions detailed in Section 2.1.5. To generalize the function, we normalize the yield by dividing it by the vertices of the fitted parabolic curves. The fitted vertex represents the maximum crop yield (Y_{max} [bu/m^2]) used in the model. Similarly, we adjust the applied water data by the maximum applied water (AW_{max} [cm]) obtained from the data. Additionally, we introduce a lower cap for the yield; if the yield falls below a threshold y_{min} [-] then the field has zero crop yield. The threshold, y_{min}, can be determined from observational data (e.g., **Text S1**). Consequently, the yield (Y [bu/m^2]) can be calculated as follows:

$$Y_c = y_c \times Y_{c,max} \tag{3}$$

$$\begin{cases} y_c = (a_c \bullet aw_c^2 + b_c \bullet aw_c + c_c) & if\ y_c \geq y_{min,c} \\ y_c = 0 & otherwise \end{cases} \tag{4}$$

$$aw_c = \frac{AW_c}{AW_{max,c}} \tag{5}$$

where the subscript c indicates crop-specific value. Terms y and aw are normalized crop yield [-] and applied water [-], respectively. Coefficients a_c, b_c, and c_c describe the shape of the water-yield production function for crop c. PyCHAMP users have the option to divide a field into several area splits for the purpose of growing mixed crops in one field.

The daily pumping rate is essential in calculating the energy requirement in the well module. Therefore, we downscale the annual withdrawal (PW [10^4 m^3] to the daily pumping rate (q [10^4 m^3/day]) by:

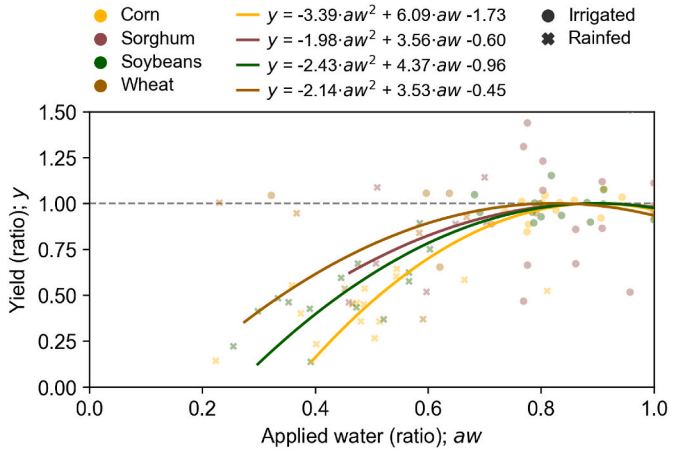

Fig. 2. Fitted yield-water production functions. The data points represent observed yields for wheat (brown), corn (yellow), sorghum (maroon), and soybeans (green) with corresponding management practices (irrigated: circles, rainfed: crosses).

$$q_w = a_{te} \bullet PW_w + b_{te} \tag{6}$$

where the subscript w denotes the well-specific values. Terms a_{te} and b_{te} are linear regression coefficients estimated from observed data for irrigation technology te.

2.1.3. Well component

The well component (module) is constructed to simulate energy use for pumping at each time step. Currently, the provided agent type in the well component is called Well class. The Well class calculates the energy (E [petajoules; PJ]) required to elevate and pressurize the volume of water pumped on an annual basis (McCarthy et al., 2020).

$$E_w = \rho \bullet g \bullet PW_w \bullet L_{T,w} \bullet \frac{1}{\varepsilon_p} \times 10^{-11} \tag{7}$$

where ρ is the density of water [kg/m^3], g is the acceleration due to gravity [m/s^2], ε_p [-] is the pumping efficiency, and 10^{-11} is for unit conversion [joule $\bullet$ 10^4 m^3 to PJ $\bullet$ m^3]. The total effective lift (L_T [m]) is equal to:

$$L_T = L_{WT} + (L_{CD} + L_{WD}) + L_{PR} \tag{8}$$

where L_{WT} [m] denotes the lift from the water table to the ground surface at the onset of the pumping season; L_{CD} [m] represents the additional lift required due to the cone of depression forming adjacent to the well screen throughout the pumping season; L_{WD} [m] signifies the added lift needed owing to drawdown within a well, a consequence of frictional losses in and around the immediate area of the well; and L_{PR} [m] reflects the effective lift necessitated by the pressurization of water and the losses in the piping associated with each type of irrigation system. We adopt the Cooper-Jacobs method and well efficiency to dynamically estimate the drawdown (i.e., $L_{CD\&WD} = L_{CD} + L_{WD}$) for each well. Well efficiency (ε_w [-]) is the ratio of the drawdown at the aquifer formation, located at the radius of the pumping well, to the total drawdown inside the well (Charbeneau, 2006).

$$L_{CD\&WD} = \frac{q}{4\pi T}\left[-0.5772 - \ln\left(\frac{r^2 S_w}{4Td}\right)\right] \times \frac{1}{\varepsilon_w} \tag{9}$$

where T is the transmissivity [m^2/day], r is the well radius [m], S_w is the specific yield of the formation in the vicinity of well w, and d is the time pumped [day]. The transmissivity can be calculated by multiplying hydraulic conductivity by the saturated thickness.

2.1.4. Finance component

The finance component (module) calculates the profit generated by specific farming practices at each time step. The current agent type available in the finance component is the Finance class. The Finance class computes profits from crop sales (R [$]), energy expenditures (C_E [$]), the operational costs of irrigation technology (C_T [$]), the operational costs of growing a certain crop (C_C [$]), and the expenses associated with transitioning to different irrigation systems (C_{dT} [$]) or crops ($C_{dC}$ [$]). Namely, the profit (*Profit* [$]) is calculated using the following equation.

$$Profit = R - (C_E + C_C + C_T + C_{dC} + C_{dT}) \tag{10}$$

where $R = Y_c \times P_c \times Area_F$ and $C_C = Y_c \times c_c \times Area_F$ are proportional to the crop yield. The terms P_c [$/bu] and c_c [$/bu] are the unit crop price and operational costs for crop c per yield, respectively. Field size is denoted as $Area_F$ [m^2]. Term C_T is a fixed cost depending on the specific irrigation technology associated with each field. The impact of different production conditions like groundwater levels is reflected in energy expenditures, C_E, like pumping cost. Transition costs, C_{dC} and C_{dT}, occur only when there are changes in the crop type grown or the irrigation technology used, respectively.

2.1.5. Behavior component

The behavior component (module) is designed to simulate farming decisions and actions, including irrigation depth, crop choice, irrigation technology choice, and water allocation strategies. The current available agent type in the behavior component is called Behavior class. Behavior class is developed following the assumption of the CONSUMAT behavioral framework with farmers' decision-making process modeled as an optimization problem. In this context, the specific farming decisions, such as crop choice, irrigation technology, and irrigation depths, are derived by employing an optimization model guided by a behavioral actor's objective. For instance, a farmer whose behaviors are driven by profit maximization will optimize their farming decisions to increase their profit returns. We organized this decision-making process into another class, called "Optimization," that allows for flexible adaptation of constraints and objectives to form an optimization model. PyCHAMP users can tailor the optimization model to fit a farmer's unique attributes, such as the field count, well count, available crop types, technological options, the time frame for decision-making (i.e., planning horizon), and policies (i.e., water rights).

2.1.5.1. CONSUMAT behavioral framework. CONSUMAT is a multi-theoretical behavioral framework used to understand and simulate individual and group behaviors, particularly in the context of consumer behavior (Jager et al., 1999). It integrates insights from psychology, sociology, and economics to explain how individuals make decisions and how these decisions can be influenced by various factors that could be tailored to fit specific cases. In our case, a behavioral actor's behaviors are categorized into four states according to satisfaction and uncertainty. Satisfaction refers to the degree to which an individual's needs and desires are met. For example, higher profits may result in greater satisfaction for a farmer. Uncertainty refers to the degree of uncertainty an individual perceives regarding their knowledge or the outcomes of their actions. For instance, a farmer might expect similar profits to those of the previous year, but the actual profit can vary due to various changing factors, including weather, market conditions, and farming practices. If a farmer is certain that the profit will fall below their satisfaction threshold, they will enter the deliberation state to optimize farming decisions, such as crop choices and irrigation depth. Otherwise, farmers will repeat the same practices (by entering the repetition state). However, if uncertainty is higher than the threshold, farmers will seek opinions from their neighbors and enter either social comparison or imitation states, depending on their level of satisfaction. The thresholds will be determined through calibration (see Section 3.3).

Mathematically, satisfaction (Sa) is defined as

$$Sa = 1 - \exp(-\alpha \times IC) \tag{11}$$

where IC is the gain like profits from the individual consumption (e.g., irrigation). The sensitivity toward such gain is governed by a factor α. A lower α means less sensitive to the given IC.

Uncertainty (Un), referring to the difference between the actual and the expected gain (e.g., expected profit solved by the optimization), is determined by taking the satisfaction anticipated in the previous timestep ($\widehat{Sa}_{t-1}$) and subtracting the actual satisfaction experienced in the current timestep (Sa_t).

$$Un_t = \widehat{Sa}_{t-1} - Sa_t \tag{12}$$

$$\widehat{Sa}_t = \frac{1}{H}\sum_{y=1}^{H} \widehat{Sa}_t^{y} \tag{13}$$

where $\widehat{Sa}_t$, is the averaged expected satisfaction over the planning horizon, H [year], and $\widehat{Sa}_t^{y}$ is the expected satisfaction for each projected year y from year t within the planning horizon. The four behavioral states in the CONSUMAT framework are repetition, deliberation, imitation, and social comparison. Within each state the behavioral actor (i.e., farmer) implements specific farming strategies like changing crop choice, irrigation technologies, and irrigation depth, as described in Table 1. We adhere to CONSUMAT's guidelines to formulate crop choice and irrigation technology decisions that typically only change under some circumstances. For example, droughts may motivate farmers to upgrade irrigation technology or grow less water-intensive crops. On the other hand, irrigation depth is annually adjusted based on climate conditions, subject to the crop choice and irrigation technology decisions. Hence, we optimize the irrigation depth in all CONSUMAT states to reflect these dynamics.

The CONSUMAT states for the initial timestep ($t = 0$) are determined using the simulation results of the initial year (i.e., prior to the start year), where Un_0 is calculated by $\widehat{Sa}_0 - Sa_0$ instead of Equation (12). In this initial step of the simulation, all farming decisions like crop types are given as inputs and only irrigation depths are optimized. Consequently, Sa_0 and Un_0 will be available for the CONSUMAT state assignment for the start year, $t = 1$.

2.1.5.2. Optimization class. The Optimization class used in the behavior module constructs an optimization problem that mirrors a farmer's attributes and their current behavioral state with a given timeframe (i.e., planning horizon). This class generates a mixed-integer nonlinear problem, containing the physical constraints outlined in Sections 2.1.2 to 2.1.**4**. These constraints are incorporated through the class's methods, such as *setup_constr_field()*, *setup_constr_well()*, and *setup_constr_finance()*. Additionally, *setup_constr_wr()* permits the PyCHAMP user to impose constraints (based on policies) on irrigation depth across all selected fields within a specified timeframe. The Optimization class streamlines the creation of optimization problems for farmers possessing diverse assets. For instance, by invoking *setup_constr_field()* twice, it's

Table 1
Definition of CONSUMAT states implemented in PyCHAMP.

State	Condition	Procedure
Repetition	$Sa > Sa_{thres}$ $Un \leq Un_{thres}$	• Repeat the chosen crop choice and irrigation technology from the previous timestep. • Optimize irrigation depth to maximize satisfaction (i.e., profit or yield).
Deliberation	$Sa \leq Sa_{thres}$ $Un \leq Un_{thres}$	• Optimize crop choice, irrigation technology, and irrigation depth to maximize satisfaction (i.e., profit or yield).
Social comparison	$Sa \leq Sa_{thres}$ $Un > Un_{thres}$	• Compare satisfaction (i.e., profit or yield) of farmer with farmer neighbors. The farmer will mimic the strategy of the neighbor with the highest satisfaction. This neighbor will also be stored in the memory for the imitation state. • Evaluate if the generated anticipated satisfaction from the selected neighbor farmer surpasses the present level of the farmer satisfaction. • If yes, then the farmer adopts the crop choice and irrigation technologies used by the selected neighbor farmer. Otherwise, no changes will be made. • Optimize irrigation depth to maximize satisfaction (i.e., profit or yield).
Imitation	$Sa > Sa_{thres}$ $Un > Un_{thres}$	• Recall the selected neighbor from its memory, otherwise randomly select one neighbor from its neighbor pool. • Evaluate if the generated anticipated satisfaction from the selected neighbor farmer surpasses the present level satisfaction of the farmer. • If yes, then the farmer adopts the crop choice and irrigation technologies used by the selected neighbor farmer. Otherwise, no changes will be made. • Optimize irrigation depth to maximize satisfaction (i.e., profit or yield).

straightforward to incorporate two unique sets of constraints and decision variables into an optimization problem, tailored for a farmer's two separate fields. Given that the groundwater level changes are the result of the total water withdrawal by a group of farmers, the projected groundwater levels of an aquifer will be used by the optimization model for each farmer to make their individual decisions. Key decision variables within the Optimization class include farmers' choices regarding irrigation depth, crop types, and irrigation technologies. PyCHAMP users can assign the objective function to maximize profit or yield via the *setup_obj()* method. The optimization problem is solved using the Gurobi solver, available for free under an academic license.

2.2. Building a simulation model using PyCHAMP

A simulation model can be created in PyCHAMP by leveraging the Mesa ABM framework. The code structure is depicted in Fig. 3, where the development of a Model class is inherited from *Mesa.Model*. The initialization process (*_init_()* method) involves setting up various agent objects, including but not limited to, Aquifer, Field, Well, Finance, and Behavior agents. These agents are then incorporated into a Mesa *scheduler* object for subsequent simulation. In addition, a Mesa *Datacollector* object is created to track output variables of interest, both at the model level and the individual agent level throughout the simulation.

The core of the simulation is the *step* method defined within the model class. This method is tasked with the regular update of agent attributes with each timestep, such as updating the crop price to reflect current market conditions. By executing the command *scheduler.step (agt_type = "Behavior")*, the simulation activates the step method for each agent classified under the "Behavior" agent type (e.g., field, well, and finance agents), allowing for the focused simulation of specific subsets of agents while still capturing other agents' dynamics through the Mesa framework. An instance of the custom Model class is created to initialize the simulation. The simulation runs by looping through the *step* method. Following agent updates, the model computes the total water withdrawal from the aquifer and invokes the aquifer objects' step method to determine the resultant changes in groundwater levels. Outputs for the current timestep are then gathered via *datacollector.collect()*. Finally, we end the simulation by calling *model.end()*, which defines actions required before closing the program for, e.g., releasing memory.

3. PyCHAMP implementation: SD-6 LEMA case study

We showcase PyCHAMP's analytical capabilities in revealing the co-evolved dynamics of human and natural systems through a case study of the SD-6 LEMA, a groundwater conservation area in the High Plains Aquifer region of northwestern Kansas (Fig. 4). This case study serves two primary objectives: 1) demonstrating the effective application of PyCHAMP, including parameterization, components connectivity, and result analysis and interpretation, and 2) illustrating the impact of network topology changes through adjustments in input files. Throughout these demonstrations, we explore the environmental and socio-economic factors that contribute to the effectiveness, adaptability, and resilience of groundwater conservation policies. Notably, the analysis incorporates a specific behavioral assumption, CONSUMAT, to examine how farmer behaviors' dynamics influence policy outcomes.

3.1. Sheridan-6 Local Enhanced Management Area

The SD-6 LEMA covers 255 km^2 (99 mi^2) in western Sheridan County and eastern Thomas County in Kansas, an area characterized by extensive groundwater irrigation, virtually no surface water, and limited groundwater recharge (Drysdale and Hendricks, 2016; Whittemore et al., 2023). This area falls within the jurisdiction of the Northwest Kansas Groundwater Management District No. 4 (KDA, 2013). The main crops grown in SD-6 LEMA are corn (averaging 74.1% of all irrigated acreage in the SD-6 LEMA for the period 2013–2020), soybean (9.3%), sorghum (8.8%), and wheat (5.1%) (USDA-NASS, 2022).

The Local Enhanced Management Area (LEMA) program was approved by the Chief Engineer of the Kansas Department of Agriculture's Division of Water Resources in late 2012 (K.S.A. 82a-1041, 2012). It was established as a tool for Groundwater Management Districts to set goals and implement measures to aid in water conservation (Marston et al., 2022). The SD-6 LEMA was the first of its kind, initially approved for a 5-year period from 2013 to 2017, and subsequently renewed for the period 2018–2022 and most recently for the period 2023–2027. The program was a collaborative effort involving local farmers. They agreed to reduce water use by 20% from their regional historical average between 2002 and 2012, allocating approximately 140 cm (55 inches) of applied water for use over a 5-year period (Griggs, 2021). The farmers' collaboration was key to the success of the program, as multiple studies have found that the irrigation water use was ~25% less during the LEMA (2013–2022) than the average from 2005 to 2012, surpassing the initial water use reduction goal and resulting in a ~65% reduction in the rate

```
Class Model(mesa.Model):
   def __init__(self, aquifer_agt_type, field_agt_type, well_agt_type,
                finance_agt_type, behavior_agt_type, settings):
      initialize aquifer, field, well, finance, and behavior agent objects
         from the assigned agent types
      create mesa scheduler and assign initialized objects to it
      define mesa datacollector
   def step(self):
      update agents' attributes
      run scheduler.step(agt_type="Behavior")
      compute total water withdrawal from an aquifer
      run scheduler.step(agt_type="Aquifer")
      collect data by datacollector.collect(self)

model = Model(settings)
for _ in length of the simulation:
   model.step()
model.end()
```

Fig. 3. A pseudocode of a general structure for a PyCHAMP simulation model. Field, well, and finance agents are executed within their respective behavior agents, to which they are assigned during initialization based on user-defined inputs.

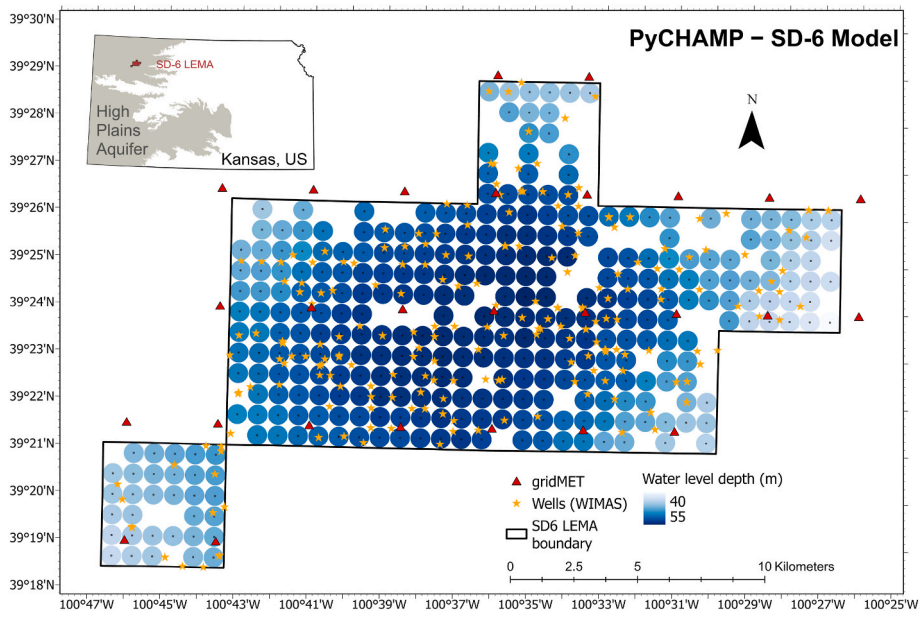

Fig. 4. The SD-6 LEMA in western Kansas. Red triangles show gridMET weather data (Abatzoglou, 2013), yellow stars mark WIMAS wells (DWR, & KGS, 2023), and blue circles represent simulated fields used by SD-6 Model, with darker blue indicating deeper average groundwater levels over 2008 to 2022.

of groundwater depletion (Butler et al., 2018; Butler and Johnson, 2024; Deines et al., 2021; Drysdale and Hendricks, 2018; Whittemore et al., 2023). Irrigation water use reductions were primarily obtained via improvements in irrigation efficiency (72% of total savings), with additional savings from shifts to lower water use crops (19%) and reductions in irrigated acreage (9%) (Deines et al., 2019), though more recently irrigated area has begun to increase (Zipper et al., 2024).

3.2. Data and SD-6 model setup

The SD-6 Model implements all default agent types across five components in PyCHAMP. We use 2007 MODFLOW simulated data (Macfarlane and Wilson, 2006) to initialize saturated thickness within a single aquifer object. The aquifer's inflow is relatively constant, where coefficients a_{aq} and b_{aq} from Equation (1) are set to 0.000376 and 0.767, respectively (Butler et al., 2018). We can calculate the groundwater levels using Equations 1 and 2. Farmers, modeled as behavior agents, make decisions about crop choice and irrigation depth over a 5-year planning horizon to maximize their averaged profit within this timeframe (i.e., the CONSUMAT objective). The annual profit is calculated through Equation (10), where the energy cost is based on the projected groundwater level. The 5-year planning horizon mirrors the LEMA governance timeframe. During the optimization at each time step, the crop choice remains fixed for the entire planning horizon while irrigation depth changes annually. In the SD-6 Model, we chose to simplify the optimization process by not incorporating uncertainties related to crop prices and future precipitation that farmers anticipate (i.e., their perceived available precipitation), assuming that both remain constant across the planning horizon. Addressing these uncertainties would necessitate a shift to a multi-stage stochastic optimization framework, which is not essential for our demonstration goal as it would significantly increase both computational time and memory requirements. However, we do integrate future groundwater levels into the optimization by projecting these levels using a linear function based on the average rate of change observed over the past five years. Also, since optimization occurs annually, only the decisions of the first year of the optimized results will be implemented, and the rest of four years will be discarded. The SD-6 Model only considers center-pivot LEPA (Low Energy Precision Application) irrigation technology, given its prevalence in the region (covering over 85% of the irrigated area from 2010 to over 96% in 2021). Crops simulated in this study include corn, sorghum, soybean, and wheat, grown on typical 50-ha (5×10^5 m^2) fields. A farmer can also choose to fallow a field. A total of 336 fields within the SD-6 LEMA were selected for inclusion in the model (Fig. 4). The fields that were not selected are typically rainfed pastures, which will not affect our study on groundwater management.

Each farmer is assumed to manage one field and a well in its center. The heterogeneous aquifer characteristics assigned to each well, such as specific yield, hydraulic conductivity, and water level depth, are determined using spatially interpolated values from Water Information Management and Analysis System's well data (WIMAS; indicated by stars in Fig. 4; DWR, & KGS, 2023). Other well properties, like well radius, are from the WIZARD statewide well database (KGS, 2023). To calculate energy consumption for pumping, we assume a pumping efficiency of 0.77, a well efficiency of 0.67, and a typical well radius of 8 inches (0.2032 m) in the region (DWR, & KGS, 2023). Additionally, we define the pumping season to be 90 days based on typical practices in the region (Table S3). In scenarios where a farmer owns multiple fields, neighbors of the farmer are defined as other farmers who have at least one field center falling within a 1-km radius of one of the fields owned by the farmer in consideration.

Along with well characteristics, additional input data includes precipitation, crop prices, energy price, initial crop types, and water-yield production functions. Precipitation data is sourced from gridMET (Abatzoglou, 2013) with each field being assigned to the nearest grid data. The Kansas Farm Management Association (KFMA) Enterprise Reports provide annual crop prices (Fig. S3; *KFMA Enterprise Reports*, 2023). Most farmers use electric pumps and we set the electricity price at $0.10 per kilowatt-hour (Find Energy LLC, 2023). Initial crop types are determined using the Cropland Data Layer (USDA-NASS, 2022), leveraging the central location of each field for extraction. Crop yields are gathered from the USDA-NASS (2022) for the selected crop types. Yield data from RMA (2023), groundwater and irrigation data from WIMAS (DWR, & KGS, 2023), and gridMET precipitation (Abatzoglou, 2013), are used to develop the water-yield production functions. The methodology for curve fitting is detailed in **Text S1**.

The simulation spans from 2008 to 2022, incorporating a 5-year pre-LEMA phase and two LEMA cycles (2013–2017 and 2018–2022) of 5-years each. The simulation schema is shown in Fig. 5. In each iteration, the model will loop over each component in PyCHAMP and update

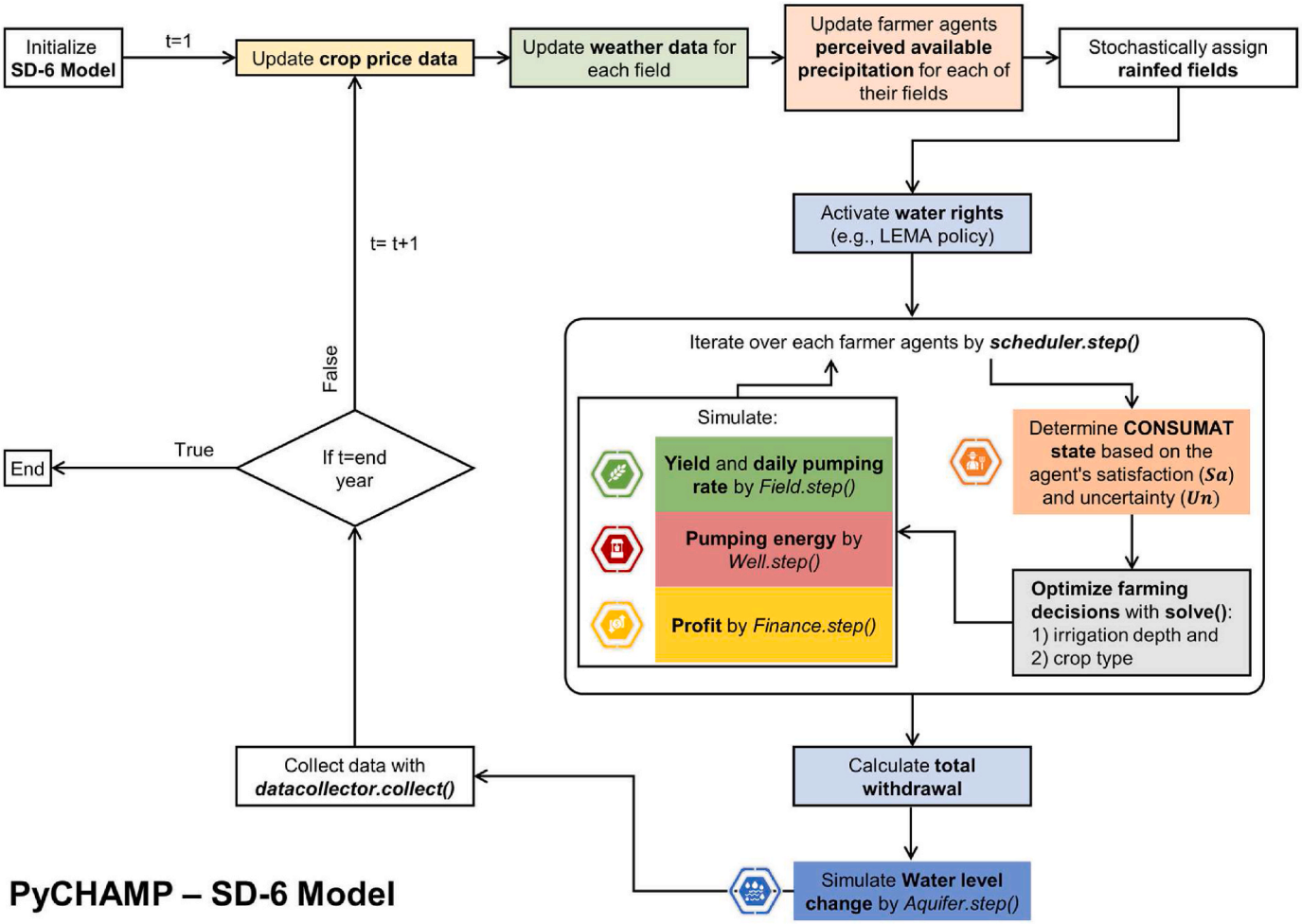

Fig. 5. Simulation schema of the SD-6 Model, developed with PyCHAMP modules within the Mesa agent-based modeling framework. The schema delineates the passing of data between components (modules) and agent types (classes), as well as the decision-making procedure of farmer agents.

corresponding agents' attributes that will influence their behavior in the next iteration, demonstrating the co-evolution of the human-water system as they respond to each other over the simulation. We start by initializing the SD-6 Model, incorporating input settings on weather, aquifers, fields, wells, finances, and farmers. Each simulation iteration begins with an update of the crop prices for the given year, reflecting the variable nature of agricultural markets. Subsequently, we refresh the weather data for each field to prepare for subsequent processes.

Farmer agents assess the perceived available precipitation for their fields using the following empirical formula derived from our own analysis and understanding of the subject, which targets to capture the bias in farmer agents' perception:

$$PAW_c = (1 - fc) \bullet p_c + fc \bullet Prec_c \tag{14}$$

$$p_c = TruncatedNormal_c^{-1}\left(qu \,\middle|\, \mu_c, \sigma_c^2, a_{tn,c}, b_{tn,c}\right) \tag{15}$$

where PAW_c represents the perceived available precipitation, p_c is the perceived risk, and $Prec_c$ is the perfect precipitation forecast for crop c during its growing season taken from gridMET (Abatzoglou, 2013) precipitation. The forecast confidence, fc, subject to calibration, abstracts various factors such as historical accuracy, personal experience with forecast reliability, and the perceived credibility of forecast sources. This variable also plays a role in correcting system bias that could occur within the calibration when multiple data sources were used to form the evaluation matric. The static perceived risk is determined by the inverse truncated normal distribution at a given quantile qu that is also subject to calibration. Parameters μ_c and σ_c^2 are the mean and variance estimated from the historical precipitation data for crop c from 2008 to 2022. The lower bound, $a_{tn,c}$, is set to be zero and the upper bound, $b_{tn,c}$, is set to be the historical maximum precipitation between 2008 and 2022.

We stochastically assign fields as rainfed, based on the historical frequency data of each field being rainfed from 2008 to 2021. However, the optimization may still output zero irrigation for fields that are not designated as rainfed if such a decision maximizes profit. For example, this could occur in years with exceptionally high precipitation where irrigation is not necessary. This approach is adopted due to our limited understanding of the factors influencing rainfed vs. irrigated field designation, which often extends beyond mere profitability. Future versions of PyCHAMP could replace this with an explicit representation of irrigation status decision-making to incorporate this into the modeling framework.

Following the determination of a field's irrigation status, the model checks the status of each water right setting and adjusts as necessary. For example, the LEMA groundwater allocation (55 inches in a 5-year time window) will only be activated starting from 2013. After these updates, the model loops through each farmer agent to determine their CONSUMAT states, optimize farming decisions, and calculate yields, energy used, and profits.

The model then computes the total groundwater withdrawal from all farmers' applied irrigation depths. Groundwater withdrawals in turn lead to groundwater level changes. A data collection process stores all relevant information before proceeding to the next iteration until the

simulation has reached its terminus. **Text S2** provides additional description of the ABM following the Overview, Design concepts, Details + Decision (ODD + D) protocol (Müller et al., 2013).

3.3. Calibration and validation

We performed a calibration and validation of our model. The simulation was divided into a calibration period (2008–2017) and a validation period (2018–2022). Four parameters were calibrated for the SD-6 Model: *qu*, *fc*, Sa_{thres}, and Un_{thres} (shared across all farmers). We adopted a particle swarm optimization algorithm (Miranda, 2018), where fifteen particles were initiated. The initial values for all four parameters were sampled by a uniform distribution within a 0 to 1 range. The objective aims to minimize the weighted root mean square error (*RMSE*), calculated as follows:

$$RMSE = 0.5 \times \left(\frac{RMSE_{st} + RMSE_{w}}{2}\right) + 0.5 \times \left(\frac{\sum_{c \in crops} RMSE_{c}}{N_{c}}\right) \quad (16)$$

where $RMSE_{st}$ is the root mean square error of the aquifer's saturated thickness, normalized by its historical maximum and minimum values. Similarly, $RMSE_{w}$ is the root mean square error of the normalized total groundwater withdrawals. The term $RMSE_{c}$ denotes the root mean square error of the distribution ratio of crop c, and N_{c} is the number of crop types. Here, we consider corn, sorghum, soybean, wheat, and fallow (thus, $N_{c} = 5$). Each particle's evaluation involved repeating the simulation three times with different random seeds (i.e., 3, 56, and 67) to account for the model's stochastic nature. The corresponding particle with parameter values, which yielded the lowest *RMSE* among the three simulations is then selected. Based on exploratory analysis, the particle swarm optimization algorithm's inertia, cognitive, and social hyperparameters were set at 0.5, 0.5, and 0.8, respectively. The algorithm was terminated when there was no improvement in 25 consecutive iterations.

3.4. Numerical experiments using the SD-6 model

To demonstrate the capabilities of PyCHAMP, we designed four numerical experiments tailored to our dual objectives of 1) demonstrating how to apply PyCHAMP, including parameterization, components connectivity, and result analysis and interpretation and 2) illustrating the impact of network topology changes through adjustments in input files. The first three experiments focus on the effective application of PyCHAMP, emphasizing parameterization, connectivity of system components, and nuanced analysis and interpretation of results. This allows us to rigorously evaluate the environmental and socio-economic factors underpinning the effectiveness of the LEMA policy, assuming the CONSUMAT framework. The fourth experiment addresses the impact of network topology changes by adjusting solely the input files without requiring additional coding. This experiment aims to reveal how modifications in network configuration influence farming decisions and water conservation behaviors, thereby providing deeper insights into the dynamic interplay between human activities and natural systems. Through this experiment design, we aim to both demonstrate PyCHAMP's utility and enhance our understanding of complex human-natural interactions.

3.4.1. Experiment 1: Quantifying the effectiveness of a water conservation policy

This experiment assesses the impact of the LEMA policy on farmer cropping patterns and irrigation decisions, and ultimately, the underlying aquifer. It is difficult to isolate the LEMA policy's effectiveness from observations alone due to uncontrolled variability in external variables, such as climate variability and economic factors. Our model allows for a more controlled experiment where we can hold external variables constant so to isolate and quantify the impact of the LEMA policy on irrigation applications, cropping patterns, and aquifer levels. More specifically, the difference between with and without LEMA policy is that the pumping is not capped to 55 inches during the 2013–2017 and 2018–2022 periods in the "No LEMA" scenario.

3.4.2. Experiment 2: Local sensitivity analysis on four calibrated parameters

Recognizing the significance of behavioral components in our model, we conducted a local sensitivity analysis on the four calibrated parameters: *qu*, *fc*, Sa_{thres}, and Un_{thres}. We perturb these parameters within a ± 0.07 range, at 0.01 intervals, to understand their influence on the model's outcomes.

3.4.3. Experiment 3: Fixed CONSUMAT state to understand behavioral dynamics in SD-6 model

To explore the impacts of behavioral dynamics, we set all farmers to operate under a fixed CONSUMAT state—either repetition, deliberation, imitation, or social comparison—throughout the simulation. This setup allows us to examine the effect of uniform behavioral strategies on model results, offering insights into the diverse ways farmers make decisions under varying conditions.

3.4.4. Experiment 4: Evaluation of pooling of groundwater and land allocations

This experiment introduces a scenario where a farmer manages three fields and three associated wells, compared to managing only one field and well in the previous experiments. We grouped three nearby fields together randomly and assigned them to a single farmer. Consequently, the number of farmers in this scenario (112) is one-third that of the original calibrated model. To assign fields and wells to a farmer, we merely need to update a farmer's input—a dictionary in Python—without modifying the underlying code. Specifically, we assign lists of corresponding field ids and well ids to the dictionary keys "*field_ids*" and "*well_ids*," respectively. Further details are available in our online manual. In addition to demonstrating the platform's flexibility in altering network topology, this scenario explores how farmers might allocate irrigation water across multiple fields and its implications for groundwater sustainability, subject to a maximum irrigation depth of 24 inches (60.96 cm) per field, as determined by pre-LEMA water rights (Kansas Department of Agriculture Division of Water Resources & U.S. Geological Survey, 2011).

4. Results

4.1. Calibration and validation

The *RMSE*, a measure that ranges from 0 (ideal) to infinity, indicates a value of 0.078 during the calibration period (2008–2018) and 0.092 for the validation period (2019–2022). These close values suggest that the calibrated model is effectively capturing the system's dynamics without being overfitted.

In-depth analysis, illustrated through Fig. 6a and b, and 7, demonstrates the model's ability to represent key variables such as saturated thickness, groundwater withdrawal, and crop ratios. The *RMSE* for each variable can be found in Table S4. These results highlight the co-evolved dynamics between human behaviors (e.g., crop selection and irrigation practices) and environmental factors (e.g., groundwater level and crop yield) in response to climate, regulatory, and economic changes. Overall, the model successfully represents the general trends observed in the SD-6 LEMA for each variable. None of the farmers in the model opt for fallowing at any point, unlike the actual SD-6 LEMA area, where 8.6% of farm fields are fallowed on average. The divergence between observations and our model suggests that decisions to leave fields fallow are likely not motivated by short-term profit but rather by crop rotation to ensure the long-term sustainability of the fields, an aspect not directly

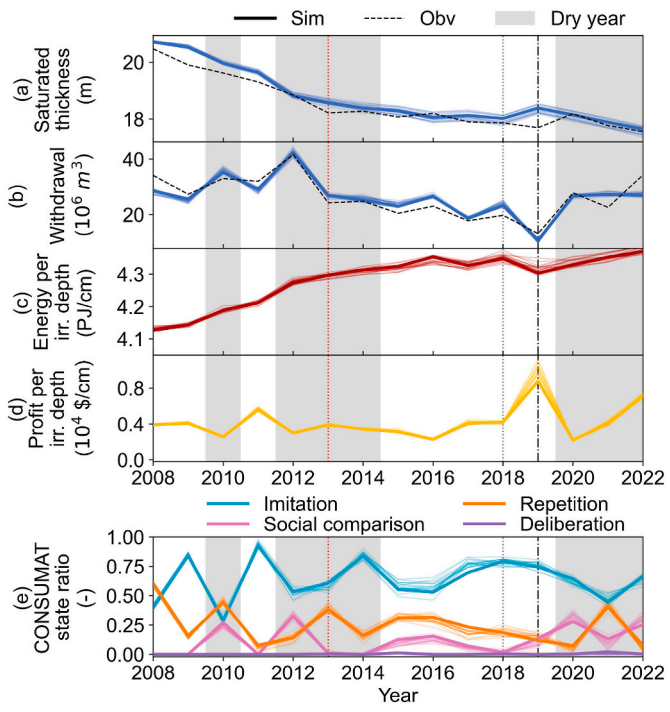

Fig. 6. Time series of a) aquifer saturated thickness, b) groundwater withdrawal, c) average energy used per irrigated depth, d) average profit per irrigated depth, and e) CONSUMAT state ratios from 2008 to 2022. The thick solid lines represent simulation results from the calibrated model, while thin solid lines represent the stochastic simulation results (20 realizations), and black dashed lines indicate the observed values. The shaded regions denote periods with annual precipitation lower than the average over the period from 2008 to 2022. The vertical red dashed line represents the start of the first LEMA period in 2013, while the dashed gray line is the start of the second LEMA period in 2018. The vertical dash-dot line separates the calibration and validation periods.

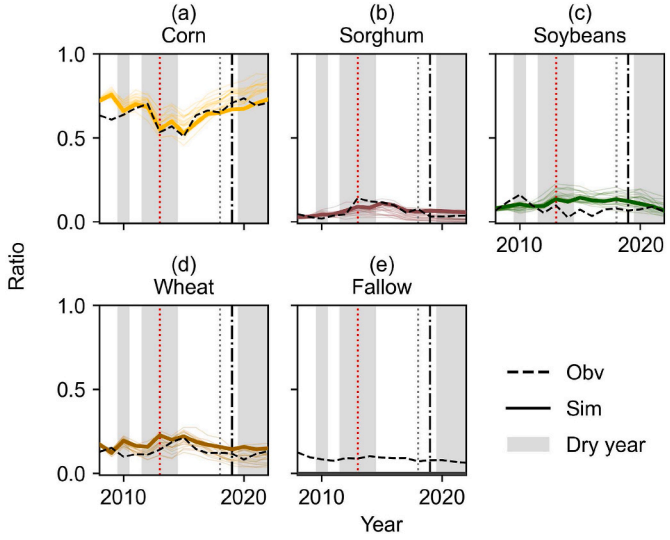

Fig. 7. Time series of crop ratios from 2008 to 2022, including a) corn, b) sorghum, c) soybeans, d) wheat, and e) fallow. The thick solid lines represent simulation results from the calibrated model, while thin solid lines represent the stochastic simulation results (20 realizations), and black dashed lines indicate the observed values. The shaded regions denote periods with annual precipitation lower than the average over the period from 2008 to 2022. The vertical red dashed line represents the start of the first LEMA period in 2013, while the dashed gray line is the start of the second LEMA period in 2018. The vertical dash-dot line separates the calibration and validation periods.

accounted for in our model. Fig. 8 reveals the spatial distribution of crop choice frequency from 2008 to 2022, demonstrating the individual-level results from PyCHAMP. The spatial patterns of crops were driven by the initial conditions, as well as the search radius used by farmers when searching for potential adaptative farming measures to mimic among their neighboring farmers. Given the complex dynamics behind the results, the actual causal relationship will require a more detailed investigation in a future study.

The versatility of PyCHAMP is further highlighted through its capability to output additional dynamics, such as energy usage, profit, and CONSUMAT state ratios, showcased in Fig. 6c, d, and 6e, respectively. The findings reveal that profit per irrigated depth improved during the second LEMA cycle, coinciding with an increase in rainfed fields, while the energy required for water pumping stabilized alongside the saturated thickness during the LEMA period.

The CONSUMAT state ratios represent the proportion of farmers in each CONSUMAT state at a given time step. The resulting state dynamics over time (Fig. 6e) shed light on the behavioral tendencies of farmers, predominantly reflecting states of imitation and repetition. These states are indicative of a generally high level of satisfaction (i.e., $Sa > Sa_{thres}$) among farmers. The alternations between imitation and repetition are primarily caused by uncertainty (i.e., *Un*), predominantly due to weather variations and crop price fluctuations. During dry years like 2010, 2012, 2020, and 2022, sudden changes in precipitation create high uncertainty and reduce satisfaction, motivating some farmers to enter the social comparison state (peaks in pink lines). The occasional entry into the deliberation state by a minority of farmers highlights the importance of initial heterogeneity in crop distribution, as most farmers adjust their farming behaviors based on their neighbors' experience. In other words, farmers showed two primary pathways to change their crop choices: they either through the optimization under the deliberation state or learn from their neighbors' experiences under the social comparison and imitation state. Given that most farmers looked to imitate their neighbor when uncertain, if the heterogeneity in crop distribution is low, farmers have fewer opportunities to learn from diverse crop choices among neighbors (i.e., all neighbors grow the same crops), which leads to decreased adaptability.

4.2. Experiment 1: Quantifying the effectiveness of a water conservation policy

With the model's credibility established through validation among multiple variables, we next explored the policy insights offered by the SD-6 Model, particularly its capacity to endogenously simulate human behaviors within the context of water conservation policies.

When simulating the 2013–2022 period without LEMA constraints, the model simulates a decrease in water withdrawals (red line in Fig. 9), though to a lesser extent than under LEMA conditions (blue line in Fig. 9). The reduction in water use under the No LEMA scenario might be due to some of the simplifying assumptions used in the model. For example, the SD-6 Model's reliance on simplified statistical assumptions, such as water-yield production functions, might not fully encapsulate the complexities of real-world scenarios, since improving irrigation efficiency would result in decreased applied water but no yield reductions if carried out effectively. This is particularly evident in the discrepancies between observed and simulated data during periods of high precipitation, indicating areas for future refinement to enhance the model's fidelity.

However, factors beyond policy, such as climatic conditions and economic shifts, can influence water use behaviors and may have contributed to the changes simulated by our model. The drought of 2012, coupled with relative price increases for crops like sorghum, soybeans, and wheat compared to corn (detailed in Fig. S3), could have encouraged some farmers within the no LEMA simulation to adopt less water-intensive crops, a behavior captured in Fig. S4. The use of the CONSUMAT framework within our model suggests that once farmers

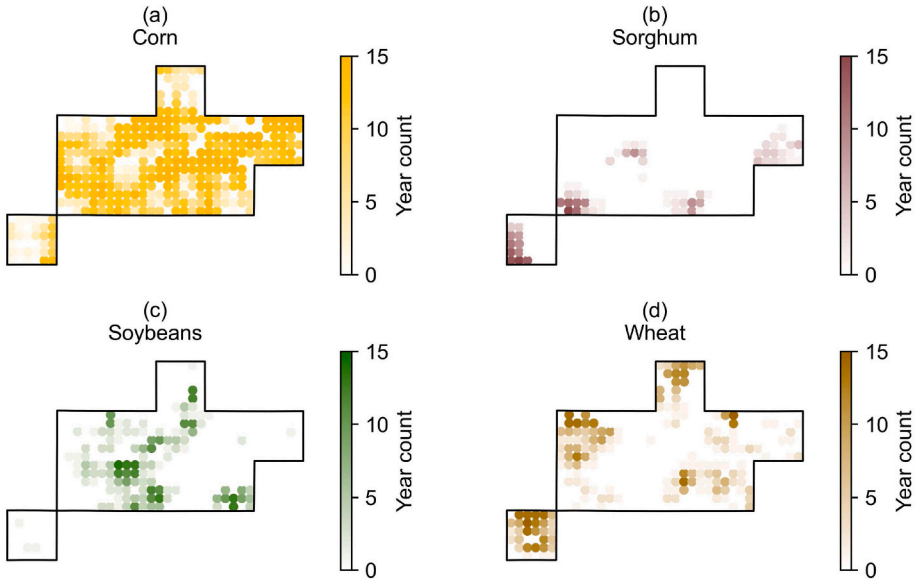

Fig. 8. Spatial distribution of crop choice frequency from 2008 to 2022 for a) corn, b) sorghum, c) soybeans, and d) wheat, based on model results.

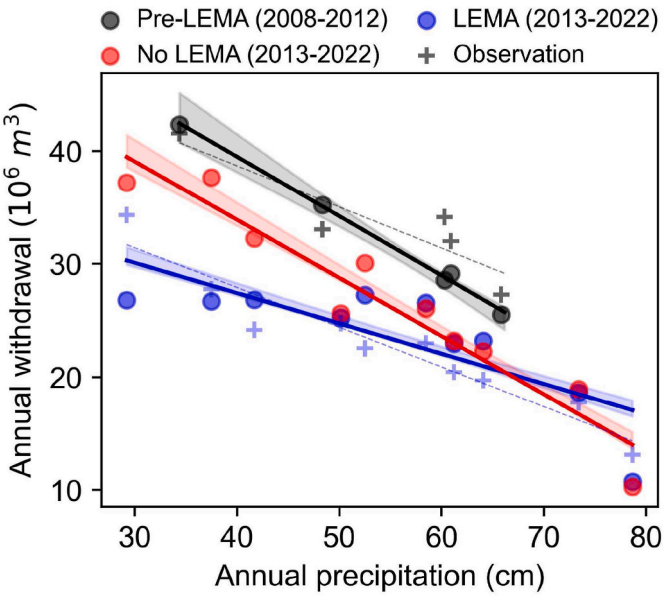

Fig. 9. A scatter plot showing the simulated results of three scenarios 1) pre-LEMA period (black), 2) LEMA period with LEMA policy (blue), and 3) a counterfactual LEMA period without LEMA policy (red). Results from each year are shown as dots, with regression lines calculated by the least square error and the bands indicating the range of ± two standard deviations over 20 realizations. The dashed lines are the regression lines using observations (+) for pre-LEMA and LEMA periods.

shifted to new crop choices due to external shocks, they were likely to adhere to these choices in the absence of further disruptions. The decrease in water withdrawals between the pre-LEMA (solid black line) and LEMA (solid blue line) was notable but since there are different economic and climatic conditions during these periods, it is difficult to assess the degree of those different factors that contribute to the change within the system. Though largely aligned, the modeled relationship between precipitation and withdrawals deviates from observations in some instances, especially during wet periods (Butler et al., 2020). Overall, however, the SD-6 Model built by PyCHAMP successfully captured the reduction in water use caused by the LEMA.

4.3. Experiment 2: Local sensitivity analysis on four calibrated parameters

Four parameters were calibrated in the SD-6 Model: quantile of perceived risks (*qu*), forecast confidence (*fc*), satisfaction threshold (Sa_{thres}), and uncertainty threshold (Un_{thres}). The quantile of perceived risks (*qu*) and forecast confidence (*fc*) mainly control the vertical shift of the withdrawal time-series. Meanwhile, the CONSUMAT thresholds for satisfaction (Sa_{thres}) and uncertainty (Un_{thres}) predominantly influence crop choice patterns. The sensitivity of the model outputs, such as water withdrawal, corn ratios, and the saturated thickness in 2022, to these behavioral parameters is shown in Fig. 10. The variables were normalized by each variable's mean value, which are called the response ratios. Corn was selected to represent the sensitivity of the crop ratios as corn is the most water-intensive and widely-grown crop compared to the others.

The analyses of boxplots in Figs. 10a and b reveal that perturbations

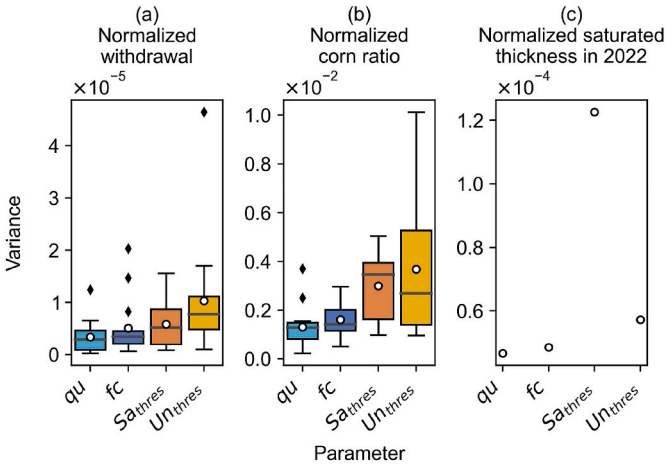

Fig. 10. Boxplots representing the variance in response ratios for, a) withdrawal, b) corn ratios, and c) saturated thickness in 2022 of the calibrated SD-6 Model (zero error bars), compared to the mean values. The local sensitivity range is set at ±0.07, in intervals of 0.01, for four calibrated parameters: the quantile of the perceived risks (*qu*), forecast confidence (*fc*), and CONSUMAT thresholds for satisfaction and uncertainty (Sa_{thres} and Un_{thres}). Diamonds are outliers.

in the parameters *qu* and *fc* induced relatively minor variances in model outputs throughout the simulation, as evidenced by the more condensed boxplots. In contrast, adjustments to the CONSUMAT thresholds not only heighten the sensitivity of the model outputs but also introduce a notable degree of variability across different years. Fig. 10c illustrates the cumulative effects of various parameters on the saturated thickness as of 2022. Given it is the results of a specific year (i.e., 2022), there are no error bars associated with it. The findings align with Figs. 10a and b revealing that CONSUMAT thresholds (Sa_{thres} and Un_{thres}) are more influential to the simulation outcomes. This variability underscores the significant role that the CONSUMAT thresholds play in driving the dynamics of the model's outputs.

4.4. Experiment 3: Fixed CONSUMAT state to understand behavior dynamics in SD-6 model

To further explore the influence of CONSUMAT framework, we examined how the system responds to farmers' behaviors when they are in a fixed CONSUMAT state throughout the simulation, as shown in Fig. 11.

First, we observe that the saturated thickness with a fixed repetition state is very close to the output from the calibrated model (Fig. 11a), but the underlying dynamics are different. Given no crop changes occur under the repetition state, the initial corn ratio (65.5%) remained the same throughout the simulations (Fig. 11b). Additionally, the irrigation depth with fixed repetition state was higher for corn and soybeans but lower for sorghum and wheat compared to the baseline model.

Second, the slight fluctuation in the corn ratio under a fixed imitation state, as seen in Fig. 11b, is attributed to farmers not having identified a neighbor to mimic yet. Consequently, they randomly selected a neighbor's crop choice to follow, as per our model's setting. The small fluctuations in the corn ratio accumulated into a distinct pattern in saturated thickness as water withdrawals varied between fixed repetition and imitation states, driven by the differences in the corn ratios. Specifically, a slightly lower corn ratio during the pre-LEMA period (2008–2012) reduces the withdrawal, especially during the dry years, leading to a lower decline in the saturated thickness.

Lastly, we found that results with fixed deliberation and social comparison states display almost identical patterns of saturated thickness in Fig. 11a, despite the distinct corn ratio patterns observed in Fig. 11b. In both scenarios, the corn ratio rapidly approached one within the first couple of years, since corn was the dominant and most profitable crop under sufficient irrigation conditions. However, the pattern of the corn ratio varied after this initial period. Farmers under the deliberation state reoptimized their crop choice annually, resulting in a lower and more variable corn ratio during dry years (shaded areas) and a higher ratio during wet years, as shown in Fig. 11b. In contrast, under the fixed social comparison state, corn dominated the region, making it less likely that farmers would learn from neighbors who grow crops other than corn. Therefore, the corn ratio remained close to 1. The change in saturated thickness depended on the amount of irrigation. In the fixed deliberation scenario, corn was the only crop irrigated. The yield of irrigated corn was around 97.35% of its maximum potential, which indicates sufficient irrigation. In the social comparison scenario, the amount of irrigated corn fields was almost the same as in the deliberation scenario. We also found the yield ratio to its maximum potential of the irrigated corn fields between deliberation and social comparison scenarios were identical. This means the water withdrawal was almost the same, leading to an overlap in patterns of saturated thickness. The differing dynamics between these two scenarios can be attributed to the crop choices in rainfed fields, which did not affect the groundwater level in our model.

4.5. Experiment 4: Evaluation of pooling of groundwater and land allocations

This experiment demonstrates the adaptable nature of model setup in PyCHAMP. By treating various elements such as fields, wells, aquifers, finances, and farmer behavior as interconnected agents within a network determined by input data, we can adjust the model setup with no changes to the source code. In this experiment, we explored a scenario comparing the impact of a behavioral actor managing three fields instead of the single field in the calibrated model. This adjustment allowed farmers to allocate water across multiple fields strategically, preferentially pumping from more productive wells and focusing their limited water resources on irrigated corn fields while choosing less water-intensive crops like sorghum, soybeans, wheat, or even leaving some fields fallow.

The results, illustrated in Fig. 12a, show a tendency among most farmers to adopt a mixed-cropping approach, balancing between maximizing corn cultivation and integrating water-saving crops to optimize water use. This mixed strategy led to higher profits during dry years (Fig. 12b), though it results in lower profits in wetter years. Economically, this approach significantly reduced profit disparities among farmers, as shown in Fig. 12c. Another observation is that the inclination to grow corn across all three fields increased, correlating

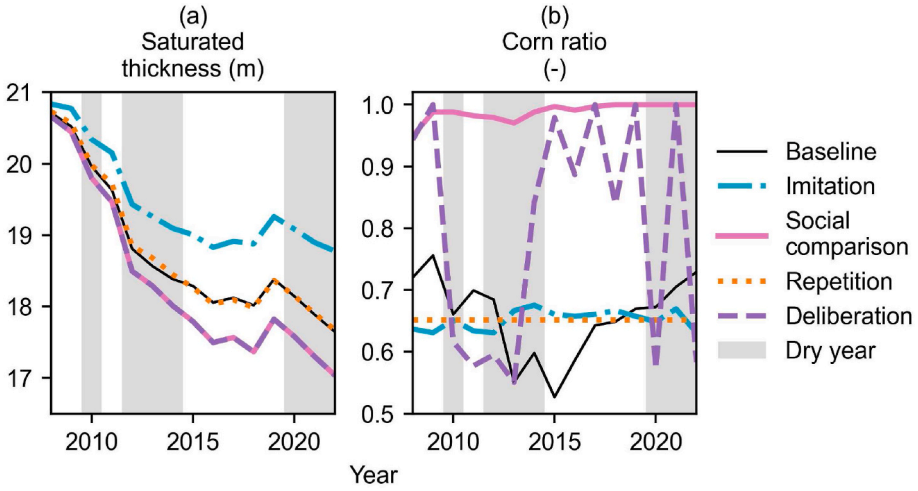

Fig. 11. Simulated a) saturated thickness and b) corn ratio under fixed CONSUMAT states: repetition (orange), deliberation (purple), imitation (cyan), and social comparison (pink). The baseline (black) is represented by the simulation of the baseline model. Shaded areas denote periods with annual precipitation lower than the average over the period from 2008 to 2022.

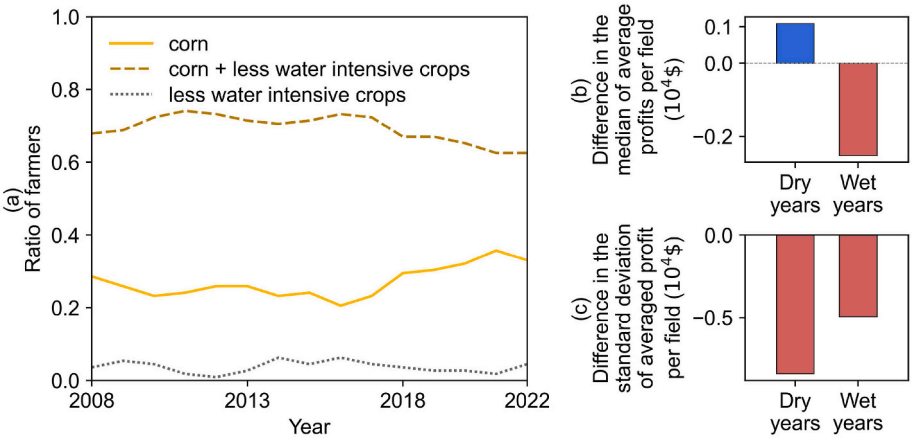

Fig. 12. a) The ratio of farmers based on crop composition across three fields is analyzed. Less water-intensive options include sorghum, soybeans, wheat, and fallow. Bar plots illustrate the values of three-field minus single-field scenarios in terms of their b) median and c) standard deviation of average profit per field during dry and wet years.

with the period of higher rainfall from 2015 to 2019 and the subsequent rise in corn prices post-2020. This trend echoes findings from the calibrated model, as well as observation, as seen in Fig. 7. When land and water resources are pooled, water withdrawals largely increase during dry years and decrease during wet years when compared to the management of a single field.

While the experiment highlights PyCHAMP's adaptability, it also reveals that computational time can escalate dramatically, ranging from a few minutes in a single-field scenario to several hours in a three-field scenario, due to the increased complexity of the optimization problems.

5. Discussion

5.1. Synthesis across four numerical experiments

The SD-6 LEMA is a uniquely successful groundwater conservation area, with significant reductions in pumping that were achieved through an irrigator-designed program (Marston et al., 2022; Whittemore et al., 2023). As such, it represents a logical testbed to explore PyCHAMP's ability to assess impacts of policy, regulations, or network topology on farmer behavior and aquifer levels. We implemented a set of four experiments to assess the potential impacts of different social and environmental factors on groundwater conservation effectiveness and the parameterization of agents in the SD-6 model. These are meant to both demonstrate PyCHAMP's capabilities, identify areas of needed future model development, and highlight key factors that could be explored through more detailed study in future work.

Experiment 1 emphasized the challenge of disentangling the impacts of policy effects from external factors, as the model captured a decrease in water withdrawal even without the LEMA policy, likely attributed to model structure, weather, and/or economic changes. However, the discrepancy from the annual withdrawal observation, particularly during high precipitation years, underscores the necessity for more in-depth analysis with more finely tuned sub-models.

Experiment 2 highlighted the notable effect of CONSUMAT threshold parameters on the model's outcomes, pointing to the importance of grounding these parameters in empirical evidence through surveys and behavioral experiments. This step is critical for enhancing the accuracy of behavioral assumptions within the model, and suggests that future modeling efforts would benefit from more closely coupled integration between social and physical science research.

In Experiment 3, the exploration of fixed CONSUMAT states unveiled complex behavioral dynamics among farmers, revealing varied decision-making processes under different scenarios. This complexity suggests that incorporating different social-behavioral theories could provide a more nuanced understanding of human behavior in system models, potentially addressing the concerns raised in Experiment 1 regarding the true effectiveness of the LEMA policy by more accurately capturing human behaviors.

Experiment 4 demonstrated PyCHAMP's flexibility by simulating a scenario in which farmers manage multiple fields. This led to the adoption of mixed-cropping strategies, a change in withdrawals during wet/dry years, and a reduction in profit disparities among farmers. Our findings support empirical evidence that farm size and groundwater use are causally linked (Ao et al., 2021). Pooling land and water among three fields resulted in longer simulation times due to the complexity of optimizing multiple fields—a factor that requires consideration in future applications.

Collectively, these experiments highlight the ability of PyCHAMP to evaluate a variety of different policies, management, and behavioral scenarios. However, they also demonstrate a need for continued integration of detailed sub-models, systematic characterization of model structural uncertainty, and refinement of behavioral parameters through empirical research. Additionally, future explorations could investigate optimal irrigation strategies under LEMA policies, account for crop insurance considerations, and address epistemic uncertainty in the behavioral framework.

5.2. Strengths and capabilities of PyCHAMP

PyCHAMP is a versatile platform featuring predefined components (modules) that reduce the technical skill requirements while retaining flexibility for users to customize agent types (classes), in which models different in simulation procedures or coupling structures can also be built following Mesa's guideline. We showcased PyCHAMP's capabilities and flexibility through the application of the SD-6 Model. This model is particularly effective in evaluating the efficacy of water conservation policies, such as the SD-6 LEMA. Unlike other agent-based agro-hydrological models (Castilla-Rho et al., 2015; Jaxa-Rozen et al., 2019; Nozari et al., 2023; Rouhi Rad et al., 2020) with rigid structural designs and limited sub-model options, PyCHAMP offers greater adaptability and applicability that enables its broader use beyond a limited geographical area or a single use case, while more constrained than Pynsim (Knox et al., 2018) to reduce technical requirement. This restricted generalizability provides several advantages over existing tools.

First, PyCHAMP maintains the flexibility to tailor model complexity to align with the user's specific research needs, data availability, and computational capabilities. This flexibility is exemplified by the possibility of incorporating more detailed physically-based hydrological

models (Aghaie et al., 2020a; Du et al., 2022; Khan and Brown, 2019; Noël and Cai, 2017) or advanced crop models such as Aquacrop-OS (Foster et al., 2017) with granular simulation timesteps through the addition of custom classes. However, additional model complexity may induce tradeoffs by creating increased model error due to propagation of uncertain process representations through highly parameterized models (Saltelli et al., 2019), so should be done with caution, only when necessary for the question or region under investigation, and only where sufficient data exist to accurately parameterize these complex models. To integrate more detailed models, the Mesa scheduler may call each agent annually (as defined in the model), but the sub-model can run in a finer step (e.g., daily) upon an annual call, or it can skip a call by customizing the associated class with an "if statement," since the "current timestep" is a global attribute available to all agents. This integration could facilitate nuanced analyses of well capacity's effects on water use (Hrozencik et al., 2017) and the evaluation of irrigation scheduling on crop yields (Jimenez et al., 2020). Once new agent types are developed and added to their corresponding component in PyCHAMP, users may then interchange agent types for a selected model (e.g., the SD-6 Model). This capability can enrich the research process by enabling an exploration of the effects of model complexity on outcomes, a fundamental and important aspect of complex system modeling (Saltelli et al., 2019).

Second, PyCHAMP supports the exploration of social-behavioral theories and the quantification of structural uncertainty in human model design. Our experiments demonstrated how the CONSUMAT behavioral framework significantly influenced modeling outcomes and the potential lock-in to a specific CONSUMAT state. Despite this, the certainty of such assumptions in the decision-making process remains low due to limited knowledge of human behaviors. PyCHAMP allows users to create diverse behavioral agent types based on various heuristics, observations, or theories like the Theory of Planned Behavior (Ajzen, 1991), facilitating the investigation of different human behavior on feedback and other complex dynamics of human-natural systems (Ekblad and Herman, 2021; Lin and Yang, 2022; Yoon et al., 2023).

Third, PyCHAMP implicitly forms a network topology over agents through user-defined inputs. Namely, this feature conceptually forms a node-link model structure similar to Pynsim (Knox et al., 2018). As opposed to grid-based models, node-link structures enable applying multiple spatial resolutions to different agent types. This approach reduces unnecessary complexity and computational costs associated with grid-based models, where the minimal spatial unit is uniformly applied (de Bruijn et al., 2023). By allowing varied spatial units across agent types, PyCHAMP enables effective information flow among components at different scales, making it an excellent tool for assessing impacts on environmental and socio-economic heterogeneity.

Lastly, leveraging the agent-based modeling framework from Mesa, PyCHAMP can evaluate policies at both the system and individual levels. This feature facilitates the exploration of equality issues (Koebele et al., 2023) among heterogeneous farmer agents, in addition to achieving systemic goals like mitigating groundwater depletion.

5.3. Limitations

While PyCHAMP offers a powerful platform for exploring human-natural systems, several limitations should be addressed in future iterations. Although PyCHAMP allows for complete flexibility in structuring simulation models with customized classes (agent types) for each component (module), it requires some programming expertise from users. However, once new models and agent types are developed and added into PyCHAMP, users can switch across them and modify the network connectivity through inputs with further code modification. To assist newcomers, we offer an online tutorial and examples at https://dises-pychamp.readthedocs.io/. Additionally, the computational cost of the optimization component can be significant, influenced by the number of behavioral actors (e.g., farmers) and input dimensions, such as the number of crop choices, technology options, fields, and wells. This arises from formulating farmers' decision-making processes as mixed-integer nonlinear problems. Solutions might include simplifying or linearizing the optimization problem, or running the model on a computing cluster to enhance scalability. Complex system modeling often requires extensive input data, and PyCHAMP may pose challenges in settings where data availability is limited. However, its modular structure is designed to maximize flexibility, allowing users to adapt the model to available data, thereby mitigating potential limitations related to data scarcity.

The SD-6 Model, which demonstrates PyCHAMP capabilities, captures dynamics related to saturated thickness, withdrawal, and crop choice. This model also allows us to highlight some assumptions and limitations that users may encounter when building models with PyCHAMP. First, the SD-6 LEMA case study presumes static inflow into the aquifer, employing constant coefficients a_{aq} and b_{aq} for the Kansas Geological Survey–Water Balance Method, which is consistent with long-term field observations in the SD-6 LEMA (Whittemore et al., 2023). However, this assumption may be problematic for simulations projecting multiple decades into the future, as the aquifer water balance could vary with increasing water use efficiency due to changes in recharge or lateral flows (Butler et al., 2020). These potential future changes to net inflow will be apparent through deviations in the Kansas Geological Survey-Water Balance Method, and therefore can be addressed by continuing to update these relationships through time. For forecasting purposes, PyCHAMP could also be modified by using dynamic inflow in the default Aquifer class (similar to Butler et al., 2020) or developing a new agent type to incorporate more complex physical groundwater models. Secondly, the static water-yield production functions used in the Field class do not consider the impacts of over-irrigation, the results of optimization, or the inter-seasonal weather variations, as evidenced by significant data uncertainty in function fitting (Fig. S2). Future integration with a more detailed crop model, such as AquaCrop-OS (Foster et al., 2017), may overcome these issues. Third, we applied uniform pumping and well efficiencies across all wells in the case study, along with consistent pumping durations. This approach fails to fully capture the heterogeneity of wells and disregards irrigation schedules. Addressing this requires simulations with finer temporal resolution, particularly for identifying optimal sub-annual irrigation strategies under LEMA policy. Fourth, the current Financial class omits considerations of crop insurance, which could influence farmers' decisions (Ghosh et al., 2023; Yu and Sumner, 2018; Zipper et al., 2024). Also, future work should further evaluate the epistemic uncertainty and quantify the model structure uncertainty associated with the 'CONSUMAT' approach adopted by the Behavior class. Finally, the assumption of annual decision-making might overlook the impact of seasonality, leading to an inaccurate representation. Future studies are encouraged to explore a finer decision-making timescale, as multiple decision points could exist, especially in cases of crop failures due to extreme weather.

6. Conclusion

In this paper, we introduce the open-source Python-based Crop-Hydrological-Agent Modeling Platform (PyCHAMP). PyCHAMP is designed to represent the complexities of human-water systems and support agricultural water management and policy modeling. The modularized components of PyCHAMP offer great flexibility and adaptability for custom applications. Specifically, PyCHAMP encompasses five main components: aquifer, field, well, finance, and behavior, which enable users to construct an interconnected complex system to explore the interplay between human and natural systems, considering both environmental and socio-economic factors.

In the SD-6 LEMA case study, we use PyCHAMP to build the SD-6 Model, successfully capturing observed dynamics in saturated thickness, groundwater withdrawal, and crop plantings. Our findings

illustrate the pivotal role of endogenously simulated human decision-making in evaluating the effectiveness of water conservation policies. The local sensitivity analysis further illuminates the significant influence of behavioral parameters on the modeling outcomes. Additionally, we explore how each CONSUMAT state affects farmers' decision-making dynamics. Our analysis also demonstrates that, during dry periods, farmers managing three fields achieve higher profits and more equitable earnings compared to the scenario where farmers manage a single field. These numerical experiments demonstrate how PyCHAMP can facilitate scenario-based analysis.

In conclusion, PyCHAMP serves as a potentially valuable tool in supporting the development and evaluation of sustainable groundwater management efforts. Its structural design not only suits current applications but also paves the way for future integrations with more sophisticated sub-models as new agent types. This facilitates exploration of coevolution theories in human-natural systems and a systematic approach to quantify model structural uncertainty, providing a new platform for future research and policymaking in agricultural groundwater management.

Software and data availability

Name of software: PyCHAMP v1.0.0.

Developers: Chung-Yi Lin and Maria Elena Orduna Alegria.

Year first available: 2024.

Program language: Python.

Operating systems supported: Windows.

Hardware required: Basic computer with 4 GB RAM and dual-core CPU.

Software or environment requirements: Python $\geq$ 3.11, Mesa $=$ 2.1.1, and Gurobi $\geq$ 11.0.2

Program size: 3 MB.

Availability: PyCHAMP v1.0 can be freely accessed on GitHub (https://github.com/philip928lin/PyCHAMP), where the user manual and data used in this manuscript are also included.

CRediT authorship contribution statement

Chung-Yi Lin: Writing – review & editing, Writing – original draft, Visualization, Validation, Software, Methodology, Investigation, Formal analysis, Data curation, Conceptualization. **Maria Elena Orduna Alegria:** Writing – review & editing, Writing – original draft, Validation, Methodology, Data curation, Conceptualization. **Sameer Dhakal:** Writing – review & editing, Software. **Sam Zipper:** Writing – review & editing, Supervision, Resources, Project administration, Funding acquisition, Conceptualization. **Landon Marston:** Writing – review & editing, Supervision, Resources, Project administration, Methodology, Funding acquisition, Conceptualization.

Declaration of competing interest

The authors declare no competing financial interests or personal relationships that could appear to influence the work reported in this paper.

Data availability

The code, user manual, and data used in this study are freely distributed on GitHub (https://github.com/philip928lin/PyCHAMP).

Acknowledgments

We would like to extend special thanks to Blake B. Wilson for providing the WIMAS and WIZARD data. The authors would like to thank the editors and two anonymous reviewers for their suggestions to improve the quality of the manuscript.

This work was supported by the National Science Foundation Grant No. RISE-2108196 ('DISES: Toward resilient and adaptive community-driven management of groundwater dependent agricultural systems') and the Foundation for Food and Agriculture Research Grant No. FF-NIA19-0000000084. Any opinions, findings, and conclusions or recommendations expressed in this material are those of the author(s) and do not necessarily reflect the views of the National Science Foundation or the Foundation for Food and Agriculture Research.

Appendix A. Supplementary data

Supplementary data to this article can be found online at https://doi.org/10.1016/j.envsoft.2024.106187.

References

Abatzoglou, J.T., 2013. Development of gridded surface meteorological data for ecological applications and modelling. Int. J. Climatol. 33 (1), 121–131. https://doi.org/10.1002/joc.3413.

Acosta-Michlik, L., Espaldon, V., 2008. Assessing vulnerability of selected farming communities in the Philippines based on a behavioural model of agent's adaptation to global environmental change. Global Environ. Change 18 (4), 554–563. https://doi.org/10.1016/j.gloenvcha.2008.08.006.

Aeschbach-Hertig, W., Gleeson, T., 2012. Regional strategies for the accelerating global problem of groundwater depletion. Nat. Geosci. 5 (12) https://doi.org/10.1038/ngeo1617. Article 12.

Aghaie, V., Alizadeh, H., Afshar, A., 2020a. Agent-Based hydro-economic modelling for analysis of groundwater-based irrigation Water Market mechanisms. Agric. Water Manag. 234, 106140 https://doi.org/10.1016/j.agwat.2020.106140.

Aghaie, V., Alizadeh, H., Afshar, A., 2020b. Emergence of social norms in the cap-and-trade policy: an agent-based groundwater market. J. Hydrol. 588, 125057 https://doi.org/10.1016/j.jhydrol.2020.125057.

Ajzen, I., 1991. The theory of planned behavior. Organ. Behav. Hum. Decis. Process. 50 (2), 179–211. https://doi.org/10.1016/0749-5978(91)90020-T.

Al-Amin, S., Berglund, E.Z., Larson, K.L., 2015. Agent-based modeling to simulate demand management strategies for shared groundwater resources, 2067–2072. https://doi.org/10.1061/9780784479162.203.

An, L., Grimm, V., Sullivan, A., Turner II, B.L., Malleson, N., Heppenstall, A., Vincenot, C., Robinson, D., Ye, X., Liu, J., Lindkvist, E., Tang, W., 2021. Challenges, tasks, and opportunities in modeling agent-based complex systems. Ecol. Model. 457, 109685 https://doi.org/10.1016/j.ecolmodel.2021.109685.

Ao, Y.Z., Hendricks, N.P., Marston, L.T., 2021. Growing farms and groundwater depletion in the Kansas High Plains. Environ. Res. Lett. 16 (8), 084065 https://doi.org/10.1088/1748-9326/ac1816.

Avisse, N., Tilmant, A., Rosenberg, D., Talozi, S., 2020. Quantitative assessment of contested water uses and management in the conflict-torn yarmouk river basin. J. Water Resour. Plann. Manag. 146 (7), 05020010 https://doi.org/10.1061/(ASCE)WR.1943-5452.0001240.

Berglund, E.Z., 2015. Using agent-based modeling for water resources planning and management. J. Water Resour. Plann. Manag. 141 (11), 04015025 https://doi.org/10.1061/(ASCE)WR.1943-5452.0000544.

Bhattarai, N., Pollack, A., Lobell, D.B., Fishman, R., Singh, B., Dar, A., Jain, M., 2021. The impact of groundwater depletion on agricultural production in India. Environ. Res. Lett. 16 (8), 085003 https://doi.org/10.1088/1748-9326/ac10de.

Butler, J.J., Bohling, G.C., Perkins, S.P., Whittemore, D.O., Liu, G., Wilson, B.B., 2023. Net inflow: an important target on the path to aquifer sustainability. Groundwater 61 (1), 56–65. https://doi.org/10.1111/gwat.13233.

Butler, J.J., Bohling, G.C., Whittemore, D.O., Wilson, B.B., 2020. Charting pathways toward sustainability for aquifers supporting irrigated agriculture. Water Resour. Res. 56 (10), e2020WR027961 https://doi.org/10.1029/2020WR027961.

Butler, J.J., Johnson, C.K., 2024. Groundwater depletion: a global challenge for intergenerational equity. Interpretation 78 (1), 7–18. https://doi.org/10.1177/00209643231201998.

Butler, J.J., Whittemore, D.O., Wilson, B.B., Bohling, G.C., 2018. Sustainability of aquifers supporting irrigated agriculture: a case study of the High Plains aquifer in Kansas. Water Int. 43 (6), 815–828. https://doi.org/10.1080/02508060.2018.1515566.

Canales, M., Castilla-Rho, J., Rojas, R., Vicuña, S., Ball, J., 2024. Agent-based models of groundwater systems: a review of an emerging approach to simulate the interactions between groundwater and society. Environ. Model. Software 175, 105980. https://doi.org/10.1016/j.envsoft.2024.105980.

Castilla-Rho, J.C., Mariethoz, G., Rojas, R., Andersen, M.S., Kelly, B.F.J., 2015. An agent-based platform for simulating complex human–aquifer interactions in managed groundwater systems. Environ. Model. Software 73, 305–323. https://doi.org/10.1016/j.envsoft.2015.08.018.

Castilla-Rho, J.C., Rojas, R., Andersen, M.S., Holley, C., Mariethoz, G., 2017. Social tipping points in global groundwater management. Nat. Human Behav. 1 (9), 640–649. https://doi.org/10.1038/s41562-017-0181-7.

Castro, J., Drews, S., Exadaktylos, F., Foramitti, J., Klein, F., Konc, T., Savin, I., van den Bergh, J., 2020. A review of agent-based modeling of climate-energy policy. WIREs Climate Change 11 (4), e647. https://doi.org/10.1002/wcc.647.

Charbeneau, R.J., 2006. Groundwater Hydraulics and Pollutant Transport. Waveland Press.
Daly, A.J., De Visscher, L., Baetens, J.M., De Baets, B., 2022. Quo vadis, agent-based modelling tools? Environ. Model. Software 157, 105514. https://doi.org/10.1016/j.envsoft.2022.105514.
de Bruijn, J.A., Smilovic, M., Burek, P., Guillaumot, L., Wada, Y., Aerts, J.C.J.H., 2023. GEB v0.1: a large-scale agent-based socio-hydrological model – simulating 10 million individual farming households in a fully distributed hydrological model. Geosci. Model Dev. (GMD) 16 (9), 2437–2454. https://doi.org/10.5194/gmd-16-2437-2023.
Deines, J.M., Kendall, A.D., Butler, J.J., Basso, B., Hyndman, D.W., 2021. Combining remote sensing and crop models to assess the sustainability of stakeholder-driven groundwater management in the US high Plains aquifer. Water Resour. Res. 57 (3), e2020WR027756 https://doi.org/10.1029/2020WR027756.
Deines, J.M., Kendall, A.D., Butler, J.J., Hyndman, D.W., 2019. Quantifying irrigation adaptation strategies in response to stakeholder-driven groundwater management in the US High Plains Aquifer. Env. Res. Lett. 14 (4), 044014 https://doi.org/10.1088/1748-9326/aafe39.
Drysdale, K.M., Hendricks, N.P., 2016. Effects of collective action water policy on Kansas farmers' irrigation decisions: the case of the sheridan county 6 LEMA. Arthur Capper Cooperative Center. https://agriculture.ks.gov/docs/default-source/dwr-water-appropriation-documents/accc_lema_factsheet7.pdf?sfvrsn=fcc48ac1_0.
Drysdale, K.M., Hendricks, N.P., 2018. Adaptation to an irrigation water restriction imposed through local governance. J. Environ. Econ. Manag. 91, 150–165. https://doi.org/10.1016/j.jeem.2018.08.002.
Du, E., Tian, Y., Cai, X., Zheng, Y., Han, F., Li, X., Zhao, M., Yang, Y., Zheng, C., 2022. Evaluating distributed policies for conjunctive surface water-groundwater management in large river basins: water uses versus hydrological impacts. Water Resour. Res. 58 (1), e2021WR031352 https://doi.org/10.1029/2021WR031352.
DWR, & KGS, 2023. *WIMAS*. WIMAS. https://geohydro.kgs.ku.edu/geohydro/wimas/.
Ekblad, L., Herman, J.D., 2021. Toward data-driven generation and evaluation of model structure for integrated representations of human behavior in water resources systems. Water Resour. Res. 57 (2), e2020WR028148 https://doi.org/10.1029/2020WR028148.
English, M.J., Solomon, K.H., Hoffman, G.J., 2002. A paradigm shift in irrigation management. J. Irrigat. Drain. Eng. 128 (5), 267–277. https://doi.org/10.1061/(ASCE)0733-9437(2002)128:5(267.
Find Energy LLC, 2023. Sheridan county, Kansas electricity rates & statistics. Find Energy. https://findenergy.com/ks/sheridan-county-electricity/.
Foster, T., Brozović, N., Butler, A.P., Neale, C.M.U., Raes, D., Steduto, P., Fereres, E., Hsiao, T.C., 2017. AquaCrop-OS: an open source version of FAO's crop water productivity model. Agric. Water Manag. 181, 18–22. https://doi.org/10.1016/j.agwat.2016.11.015.
Ghosh, P.N., Miao, R., Malikov, E., 2023. Crop insurance premium subsidy and irrigation water withdrawals in the western United States. Geneva Pap. Risk Insur. - Issues Pract. 48 (4), 968–992. https://doi.org/10.1057/s41288-021-00252-4.
Gorelick, S.M., Zheng, C., 2015. Global change and the groundwater management challenge. Water Resour. Res. 51 (5), 3031–3051. https://doi.org/10.1002/2014WR016825.
Griggs, B.W., 2021. Reaching Consensus about Conservation: High Plains Lessons for California's Sustainable Groundwater Management Act.
Han, Y., Mao, L., Chen, X., Zhai, W., Peng, Z.-R., Mozumder, P., 2022. Agent-based modeling to evaluate human–environment interactions in community flood risk mitigation. Risk Anal. 42 (9), 2041–2061. https://doi.org/10.1111/risa.13854.
Harbaugh, A.W., 2005. MODFLOW-2005, the US Geological Survey Modular Ground-Water Model: the Ground-Water Flow Process, 6. US Department of the Interior, US Geological Survey, Reston, VA, USA. http://wwwbrr.cr.usgs.gov/hill_tiedeman_book/documentation/MODFLOW-MODPATH-ModelViewer/MF2005-tma6a16.pdf.
Harou, J.J., Pulido-Velazquez, M., Rosenberg, D.E., Medellín-Azuara, J., Lund, J.R., Howitt, R.E., 2009. Hydro-economic models: concepts, design, applications, and future prospects. J. Hydrol. 375 (3–4), 627–643. https://doi.org/10.1016/j.jhydrol.2009.06.037.
Holtz, G., Pahl-Wostl, C., 2012. An agent-based model of groundwater over-exploitation in the Upper Guadiana, Spain. Reg. Environ. Change 12 (1), 95–121. https://doi.org/10.1007/s10113-011-0238-5.
Hrozencik, R.A., Manning, D.T., Suter, J.F., Goemans, C., Bailey, R.T., 2017. The heterogeneous impacts of groundwater management policies in the republican river basin of Colorado. Water Resour. Res. 53 (12), 10757–10778. https://doi.org/10.1002/2017WR020927.
Jager, W., Janssen, M.A., Vlek, C.A.J., 1999. Consumats in a commons dilemma. Centre for Environment and Traffic Psychology. University of Groningen, Groningen, COV, p. 55.
Jasechko, S., Seybold, H., Perrone, D., Fan, Y., Shamsudduha, M., Taylor, R.G., Fallatah, O., Kirchner, J.W., 2024. Rapid groundwater decline and some cases of recovery in aquifers globally. Nature 625 (7996). https://doi.org/10.1038/s41586-023-06879-8. Article 7996.
Jaxa-Rozen, M., Kwakkel, J.H., Bloemendal, M., 2019. A coupled simulation architecture for agent-based/geohydrological modelling with NetLogo and MODFLOW. Environ. Model. Software 115, 19–37. https://doi.org/10.1016/j.envsoft.2019.01.020.
Jimenez, A.-F., Cardenas, P.-F., Jimenez, F., Ruiz-Canales, A., López, A., 2020. A cyber-physical intelligent agent for irrigation scheduling in horticultural crops. Comput. Electron. Agric. 178, 105777 https://doi.org/10.1016/j.compag.2020.105777.
Kaiser, K.E., Flores, A.N., Hillis, V., 2020. Identifying emergent agent types and effective practices for portability, scalability, and intercomparison in water resource agent-based models. Environ. Model. Software 127, 104671. https://doi.org/10.1016/j.envsoft.2020.104671.
Kansas Department of Agriculture Division of Water Resources & U.S. Geological Survey, 2011. Kansas Irrigation Water Use 2011. Kansas Department of Agriculture. https://www.agriculture.ks.gov/home/showpublisheddocument/1898/638457633698859593.
KDA, 2013. Order of Designation Approving the Sheridan 6 Local Enhanced Management Area within Groundwater Management District No. 4. Kansas Department of Agriculture, Manhattan, KS. http://ksrevisor.org/statutes/chapters/ch82a/082a_010_0041.html.
KFMA Enterprise Reports, 2023. KFMA Enterprise Reports. https://www.agmanager.info/kfma/kfma-enterprise-reports.
KGS, 2023. *WIZARD*. WIZARD Water Well Levels Database. https://geohydro.kgs.ku.edu/geohydro/wizard/.
Khan, H.F., Brown, C.M., 2019. Effect of hydrogeologic and climatic variability on performance of a groundwater market. Water Resour. Res. 55 (5), 4304–4321. https://doi.org/10.1029/2018WR024180.
Klassert, C., Yoon, J., Sigel, K., Klauer, B., Talozi, S., Lachaut, T., Selby, P., Knox, S., Avisse, N., Tilmant, A., Harou, J.J., Mustafa, D., Medellín-Azuara, J., Bataineh, B., Zhang, H., Gawel, E., Gorelick, S.M., 2023. Unexpected growth of an illegal water market. Nat. Sustain. 6 (11), 1406–1417. https://doi.org/10.1038/s41893-023-01177-7.
Knox, S., Meier, P., Yoon, J., Harou, J.J., 2018. A python framework for multi-agent simulation of networked resource systems. Environ. Model. Software 103, 16–28. https://doi.org/10.1016/j.envsoft.2018.01.019.
Koebele, E.A., Méndez-Barrientos, L.E., Nadeau, N., Gerlak, A.K., 2023. Beyond engagement: enhancing equity in collaborative water governance. WIREs Water e1687. https://doi.org/10.1002/wat2.1687 n/a(n/a).
K.S.A. 82a-1041, 2012. 82a-1041. Local enhanced management areas; establishment procedures; duties of chief engineer*; hearing; notice; orders; review*. http://ksrevisor.org/statutes/chapters/ch82a/082a_010_0041.html.
Lall, U., Josset, L., Russo, T., 2020. A snapshot of the world's groundwater challenges. Annu. Rev. Environ. Resour. 45 (1), 171–194. https://doi.org/10.1146/annurev-environ-102017-025800.
Lin, C.-Y., Yang, Y.E., Chaudhary, A.K., 2023. Pay-for-practice or Pay-for-performance? A coupled agent-based evaluation tool for assessing sediment management incentive policies. J. Hydrol. 624, 129959.
Lin, C.-Y., Yang, Y.-C.E., 2022. The effects of model complexity on model output uncertainty in Co-evolved coupled natural-human systems—lin—2022—earth's future—wiley online library. Earth's Future 10 (6). https://doi.org/10.1029/2021EF002403.
Liu, J., Dietz, T., Carpenter, S.R., Folke, C., Alberti, M., Redman, C.L., Schneider, S.H., Ostrom, E., Pell, A.N., Lubchenco, J., Taylor, W.W., Ouyang, Z., Deadman, P., Kratz, T., Provencher, W., 2007. Coupled human and natural systems. AMBIO A J. Hum. Environ. 36 (8), 639–649. https://doi.org/10.1579/0044-7447(2007)36[639:CHANS]2.0.CO;2.
Macfarlane, P.A., Wilson, B.B., 2006. *Enhancement Of the Bedrock-Surface-Elevation Map Beneath the Ogallala Portion of the High Plains Aquifer, Western Kansas* (Technical Series 20). Kansas Geological Survey. https://www.kgs.ku.edu/Publications/Bulletins/TS20/.
Malekinezhad, H., Banadkooki, F.B., 2017. Modeling impacts of climate change and human activities on groundwater resources using MODFLOW. Journal of Water and Climate Change 9 (1), 156–177. https://doi.org/10.2166/wcc.2017.147.
Marston, L.T., Zipper, S., Smith, S.M., Allen, J.J., Butler, J.J., Gautam, S., Yu, D.J., 2022. The importance of fit in groundwater self-governance. Environ. Res. Lett. 17 (11), 111001 https://doi.org/10.1088/1748-9326/ac9a5e.
Masad, D., Kazil, J., 2015. MESA: an agent-based modeling framework. In: 14th PYTHON in Science Conference, pp. 53–60, 2015. https://citeseerx.ist.psu.edu/document?repid=rep1&type=pdf&doi=25e969b8cf94d925afc38f6cc678cf22cc523f52.
McCarthy, B., Anex, R., Wang, Y., Kendall, A.D., Anctil, A., Haacker, E.M.K., Hyndman, D.W., 2020. Trends in water use, energy consumption, and carbon emissions from irrigation: role of shifting technologies and energy sources. Environ. Sci. Technol. 54 (23), 15329–15337. https://doi.org/10.1021/acs.est.0c02897.
Mialhe, F., Becu, N., Gunnell, Y., 2012. An agent-based model for analyzing land use dynamics in response to farmer behaviour and environmental change in the Pampanga delta (Philippines). Agric. Ecosyst. Environ. 161, 55–69. https://doi.org/10.1016/j.agee.2012.07.016.
Miranda, L.J., 2018. PySwarms: a research toolkit for particle swarm optimization in Python. J. Open Source Softw. 3 (21), 433. https://doi.org/10.21105/joss.00433.
Mukherjee, A., Scanlon, B.R., Aureli, A., Langan, S., Guo, H., McKenzie, A., 2021. Chapter 1 - global groundwater: from scarcity to security through sustainability and solutions. In: Mukherjee, A., Scanlon, B.R., Aureli, A., Langan, S., Guo, H., McKenzie, A.A. (Eds.), Global Groundwater. Elsevier, pp. 3–20. https://doi.org/10.1016/B978-0-12-818172-0.00001-3.
Müller, B., Bohn, F., Dreßler, G., Groeneveld, J., Klassert, C., Martin, R., Schlüter, M., Schulze, J., Weise, H., Schwarz, N., 2013. Describing human decisions in agent-based models – ODD + D, an extension of the ODD protocol. Environ. Model. Software 48, 37–48. https://doi.org/10.1016/j.envsoft.2013.06.003.
Noël, P.H., Cai, X., 2017. On the role of individuals in models of coupled human and natural systems: lessons from a case study in the Republican River Basin. Environ. Model. Software 92, 1–16. https://doi.org/10.1016/j.envsoft.2017.02.010.
Nozari, S., Bailey, R.T., Rouhi Rad, M., Smith, G.E.B., Andales, A.A., Zambreski, Z.T., Tavakoli-Kivi, S., Sharda, V., Kisekka, I., Gowda, P., Schipanski, M.E., 2023. Capturing human-crop-groundwater interactions: modeling real-world agents in an intensively irrigated region of the U.S. High Plains (SSRN Scholarly Paper 4705465). https://doi.org/10.2139/ssrn.4705465.

Ostrom, E., 1990. Governing the Commons: the Evolution of Institutions for Collective Action. Cambridge University Press.
Ostrom, E., 2009. A general framework for analyzing sustainability of social-ecological systems. Science 325 (5939), 419–422. https://doi.org/10.1126/science.1172133.
Reed, P.M., Hadjimichael, A., Moss, R.H., Brelsford, C., Burleyson, C.D., Cohen, S., Dyreson, A., Gold, D.F., Gupta, R.S., Keller, K., Konar, M., Monier, E., Morris, J., Srikrishnan, V., Voisin, N., Yoon, J., 2022. Multisector dynamics: advancing the science of complex adaptive human-earth systems. Earth's Future 10 (3), e2021EF002621. https://doi.org/10.1029/2021EF002621.
Rouhi Rad, M., Haacker, E.M.K., Sharda, V., Nozari, S., Xiang, Z., Araya, A., Uddameri, V., Suter, J.F., Gowda, P., 2020. MOD$$AT: a hydro-economic modeling framework for aquifer management in irrigated agricultural regions. Agric. Water Manag. 238, 106194 https://doi.org/10.1016/j.agwat.2020.106194.
Saltelli, A., Aleksankina, K., Becker, W., Fennell, P., Ferretti, F., Holst, N., Li, S., Wu, Q., 2019. Why so many published sensitivity analyses are false: a systematic review of sensitivity analysis practices. Environ. Model. Software 114, 29–39. https://doi.org/10.1016/j.envsoft.2019.01.012.
Savin, I., Creutzig, F., Filatova, T., Foramitti, J., Konc, T., Niamir, L., Safarzynska, K., van den Bergh, J., 2023. Agent-based modeling to integrate elements from different disciplines for ambitious climate policy. WIREs Climate Change 14 (2), e811. https://doi.org/10.1002/wcc.811.
Schrieks, T., Botzen, W.J.W., Wens, M., Haer, T., Aerts, J.C.J.H., 2021. Integrating behavioral theories in agent-based models for agricultural drought risk assessments. Frontiers in Water 3. https://www.frontiersin.org/articles/10.3389/frwa.2021.686329.
Sivapalan, M., Savenije, H.H., Blöschl, G., 2012. Socio-hydrology: a new science of people and water. Hydrol. Process. 26 (8), 1270–1276.
Srikrishnan, V., Keller, K., 2021. Small increases in agent-based model complexity can result in large increases in required calibration data. Environ. Model. Software 138, 104978. https://doi.org/10.1016/j.envsoft.2021.104978.
Sun, Z., Lorscheid, I., Millington, J.D., Lauf, S., Magliocca, N.R., Groeneveld, J., Balbi, S., Nolzen, H., Müller, B., Schulze, J., Buchmann, C.M., 2016. Simple or complicated agent-based models? A complicated issue. Environ. Model. Software 86, 56–67. https://doi.org/10.1016/j.envsoft.2016.09.006.
Sutanudjaja, E.H., van Beek, R., Wanders, N., Wada, Y., Bosmans, J.H.C., Drost, N., van der Ent, R.J., de Graaf, I.E.M., Hoch, J.M., de Jong, K., Karssenberg, D., López López, P., Peßenteiner, S., Schmitz, O., Straatsma, M.W., Vannametee, E., Wisser, D., Bierkens, M.F.P., 2018. PCR-GLOBWB 2: a 5 arcmin global hydrological and water resources model. Geosci. Model Dev. (GMD) 11 (6), 2429–2453. https://doi.org/10.5194/gmd-11-2429-2018.
Taylor, R.G., Scanlon, B., Döll, P., Rodell, M., van Beek, R., Wada, Y., Longuevergne, L., Leblanc, M., Famiglietti, J.S., Edmunds, M., Konikow, L., Green, T.R., Chen, J., Taniguchi, M., Bierkens, M.F.P., MacDonald, A., Fan, Y., Maxwell, R.M., Yechieli, Y., et al., 2013. Ground water and climate change. Nat. Clim. Change 3 (4). https://doi.org/10.1038/nclimate1744. Article 4.
USDA-NASS, 2022. USDA national agricultural statistics service cropland data layer. USDA National Agricultural Statistics Service Cropland Data Layer. https://nassgeodata.gmu.edu/CropScape/.
Vinh, N.N.G., Tuan, L.A., Bousquet, F., 2005. Economic differentiation of rice and shrimp farming sustems and riskiness: a case of Bac Lieu, Mekong Delta, Vietnam. International Rice Research Institution. https://agritrop.cirad.fr/530532/1/ID530532.pdf.
Wada, Y., de Graaf, I.E.M., van Beek, L.P.H., 2016. High-resolution modeling of human and climate impacts on global water resources. J. Adv. Model. Earth Syst. 8 (2), 735–763. https://doi.org/10.1002/2015MS000618.
Whittemore, D.O., Butler, J.J., Bohling, G.C., Wilson, B.B., 2023. Are we saving water? Simple methods for assessing the effectiveness of groundwater conservation measures. Agric. Water Manag. 287, 108408 https://doi.org/10.1016/j.agwat.2023.108408.
Wilensky, U., 1999. NetLogo. Evanston, IL.
Wu, F., Yang, X., Cui, Z., Ren, L., Jiang, S., Liu, Y., Yuan, S., 2024. The impact of human activities on blue-green water resources and quantification of water resource scarcity in the Yangtze River Basin. Sci. Total Environ. 909, 168550 https://doi.org/10.1016/j.scitotenv.2023.168550.
Yoon, J., Wan, H., Daniel, B., Srikrishnan, V., Judi, D., 2023. Structural model choices regularly overshadow parametric uncertainty in agent-based simulations of household flood risk outcomes. Comput. Environ. Urban Syst. 103, 101979 https://doi.org/10.1016/j.compenvurbsys.2023.101979.
Yu, J., Sumner, D.A., 2018. Effects of subsidized crop insurance on crop choices. Agric. Econ. 49 (4), 533–545. https://doi.org/10.1111/agec.12434.
Zellner, M.L., 2008. Embracing complexity and uncertainty: the potential of agent-based modeling for environmental planning and policy. Plann. Theor. Pract. 9 (4), 437–457. https://doi.org/10.1080/14649350802481470.
Zhang, J., Yang, Y.C.E., Abeshu, G.W., Li, H., Hung, F., Lin, C.-Y., Leung, L.R., 2024. Exploring the food-energy-water nexus in coupled natural-human systems under climate change with a fully integrated agent-based modeling framework. J. Hydrol. 634, 131048 https://doi.org/10.1016/j.jhydrol.2024.131048.
Zipper, S., Kastens, J., Foster, T., Wilson, B.B., Melton, F., Grinstead, A., Deines, J., Butler, J., Marston, L., 2024. Estimating irrigation water use from remotely sensed evapotranspiration data: accuracy and uncertainties across spatial scales. https://eartharxiv.org/repository/view/6781/.
Zolfagharipoor, M.A., Ahmadi, A., 2021. Agent-based modeling of participants' behaviors in an inter-sectoral groundwater market. J. Environ. Manag. 299, 113560 https://doi.org/10.1016/j.jenvman.2021.113560.